Black Liquor Combustion Validated Recovery Boiler Modeling Final Year Report

Volume 5
(Appendix V)

by

T.M. Grace, W.J. Frederick, M. Salcudean, and R.A. Wessel

August 1998

A Summary Report
of the Project

Work Performed Under Contract DE-FG07-90CE40936

Prepared for

The U.S. Department of Energy
Office of Industrial Technologies
Washington, D.C.

Prepared by

The Institute of Paper Science and Technology
Atlanta, GA

Oregon State University
Corvallis, OR

University of British Columbia
Vancouver, BC, Canada

Babcock & Wilcox Company
Alliance, OH

Table of Contents
Volume 5

Appendix V

Model Validation Simulations and Comparison with Data

By

Steven J. Lien

Thomas M. Grace

Wolfgang Schmidl

Institute of Paper Science and Technology

Contents

Introduction

For three different recovery boilers, model simulations were setup and run based on the actual geometry and operating conditions of the boiler. The results of these simulations are described in the following report. For all three of these models, data was collected in an attempt to validate the results predicted by the model. In reality it was found to be very difficult to obtain data which corresponded directly to similar data from the simulation cases.

Local velocity data, which is directly calculated by these computational fluid dynamics (CFD) based models, would be the best parameter to verify the accuracy of these models. Unfortunately, velocity is extremely difficult to measure, because of the turbulent three dimensional flow pattern, and the dirty and high temperature environment of the boiler.

Local temperature measurements can be made in the boiler; however the calculated temperatures from the model are dependent on input variables which are not well known, such as the wall temperatures and radiation model variables. For these reasons temperature does not provide a good variable for gauging the accuracy of the basic model. Furthermore, even temperature measurements are difficult to obtain, due to the high temperatures which greatly reduce the lifespan of thermocouples and other types of probes and due to the effect of radiation heat transfer which reduces the accuracy of the measurements.

Most other variables have similar limitations, either in the usefulness of the data, or in the ability to accurately measure that variable. For gas composition, accurate measurements are difficult to make directly within the furnace. Accurate measurements can be made down stream at the stack, but this does not correspond directly to model predictions. In addition the gas composition predicted by the model is sensitive to the amount and location of air leaking into the boiler, which is not well known.

In general data collection in an operating recovery boiler is extremely difficult and limited by environment with in the boiler. In all cases access to the boiler is limited to small regions close to ports. The variables which are most desirable are also the most difficult to measure. Validation of the model requires making measurements over a large geographic region within the boiler, which becomes an immense undertaking.

All of the simulations were performed using a model that was developed at the University of British Columbia (UBC), especially for use with recovery boilers.

Case 1, the first recovery boiler simulation is a fairly large recovery boiler, with horizontal dimensions of 10.0 by 9.12 meters and a height of 26.0 meters from the floor to the bullnose. It has a rated capacity of 3.7×10^6 lb/day of black liquor solids and uses a two level air system.

The second recovery boiler (Case 2) is a smaller unit with a rated capacity of 1.5×10^6 lb./day of black liquor solids. The overall dimensions are 6.45 m from front to rear, 6.76 m from side to side, and a height of 17.2 m to the bullnose. This unit has been retrofitted within the last ten years and uses a three level air system.

Case 3, the last simulation was performed as a benchmarking study. The simulation was based on a physical model of an actual recovery boiler. The physical model is constructed of plexiglass and uses water to represent the air flow patterns. Laser doppler velocimetry is used to measure the velocity in the model. The measured velocity is compared to the calculated velocity.

Case 1

A set of data was collected from the Case 1 recovery boiler, as the first part of a comprehensive plan to obtain recovery boiler data for use in the validation of computer models of recovery boilers. The work was performed by two teams from the University of Toronto and the Institute of Paper Science and Technology (IPST). The University of Toronto was involved in an ongoing study of this boiler, with the primary focus on boiler plugging and fouling. During a one week test period (March 25-29, 1996) the scope of the data collection as expanded to include data useful in the overall model validation study.

The data obtained from this study can be split into two broad groups. The first set is the inlet conditions, which includes the boiler geometry and the inlet conditions for the air and black liquor flows. This data is needed to setup and run the computer simulations. The second set of outlet conditions is the data which is predicted by the models and which is needed to validate the results.

Model Setup

In 1996 a set of physical measurements were made at a recovery boiler for use in validating the predictions obtained from recovery boiler models. For this same boiler a model simulation was set-up and solved using the computational fluid dynamics (CFD) model which was developed at the University of British Columbia. The simulation was performed as a cooperative effort between IPST and UBC.

Geometry and Grid

The recovery boiler is an ABB-CE design with overall dimensions of 359 inches (9.12 m) from front to rear, 395 inches (10.0 m) from side to side, and an overall height of 1608 inches (40.8 m) as shown in Figure 1. The model was setup to include the upper furnace heat transfer regions including the superheaters and up to the center-line of the generating bank. The grid is separated into five different segments to allow for a finer grid in the lower furnace to accurately model the air ports and a coarser grid in upper furnace to reduce the computational load on the computer. The grid structure is shown in Figure 2.

The boiler uses a two-level air system. The primary ports are located at an elevation of 42 inches (1.07 m) above the floor of the boiler. There are 26 ports on both the front and rear walls and 31 ports on each side wall for a total of 114 primary air ports. The boiler also has a set of upper primaries which are not used in the current boiler operation and were not included in the model. Because of the large number of primary ports the air inlet at the primary level was modeled as a single long narrow slot for each wall. This reduced the number of cells required in the model and the computation time, while maintaining the same port area and the correct initial velocity at the primary air level.

The secondary air level is a tangential arrangement with four large ports in each corner of the boiler. These are located at an elevation of 405 inches (10.3 m). The secondary air is introduced to create a swirling pattern at this level in the boiler. Because the grid is defined on a cartesian coordinate system, the secondary ports in the model are actually defined as two ports on each of the side walls, with the initial velocity orientated to produce the correct swirling pattern. Each of the corner secondary ports actually consists of five sections aligned vertically. Three of these are open and used for air and two are closed with only a low velocity air leakage rate.

Inlet and Boundary Conditions

The recovery boiler operation is limited by plugging in the upper furnace so that the black liquor feed rate and the inlet air flow rates are almost always held at a standard condition. The model was setup to match these typical operating conditions. The air inlet velocities at all of the ports are listed below in Table 1, below.

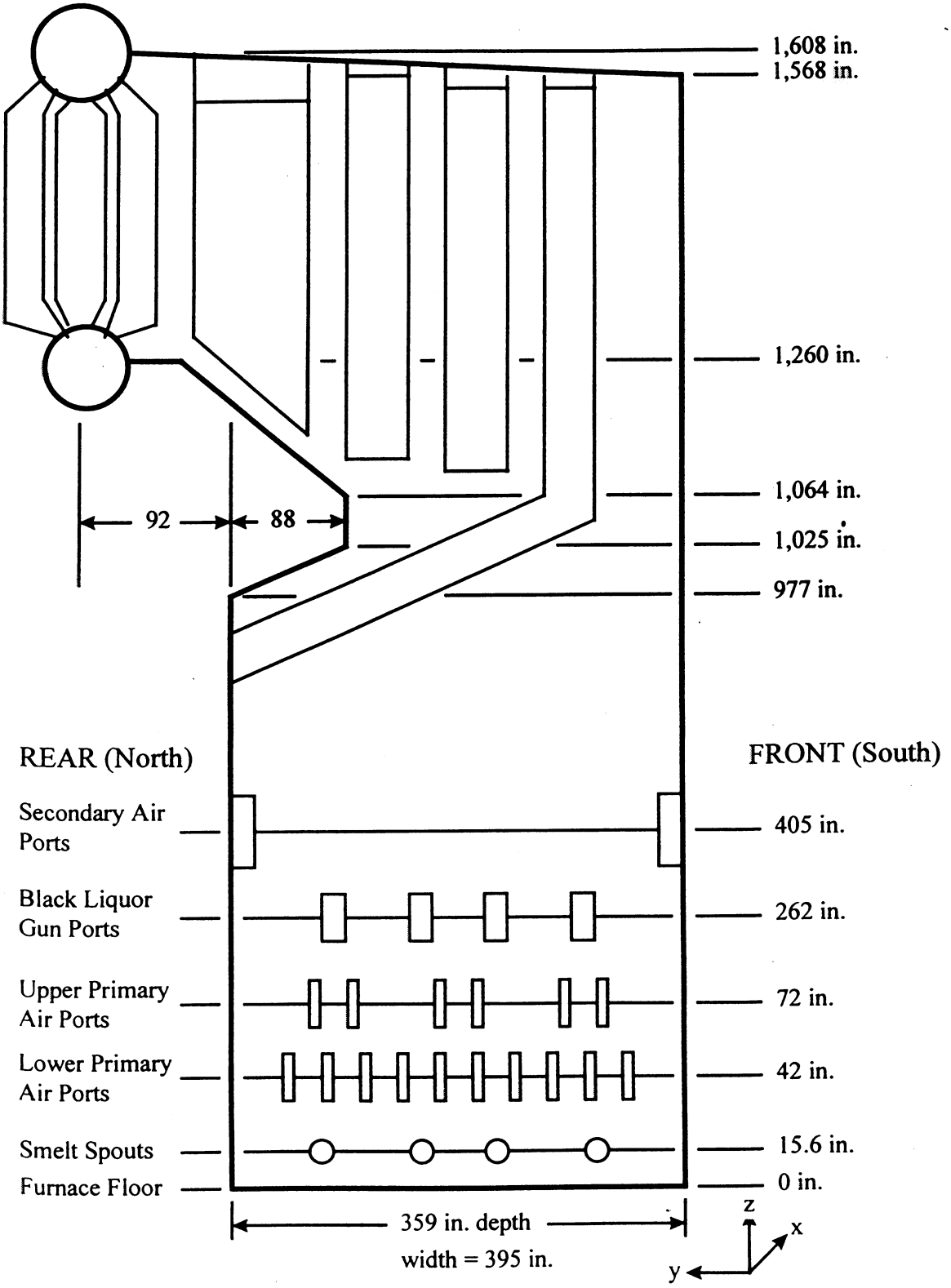

Figure 1. Geometry of Case 1 Recovery Boiler.

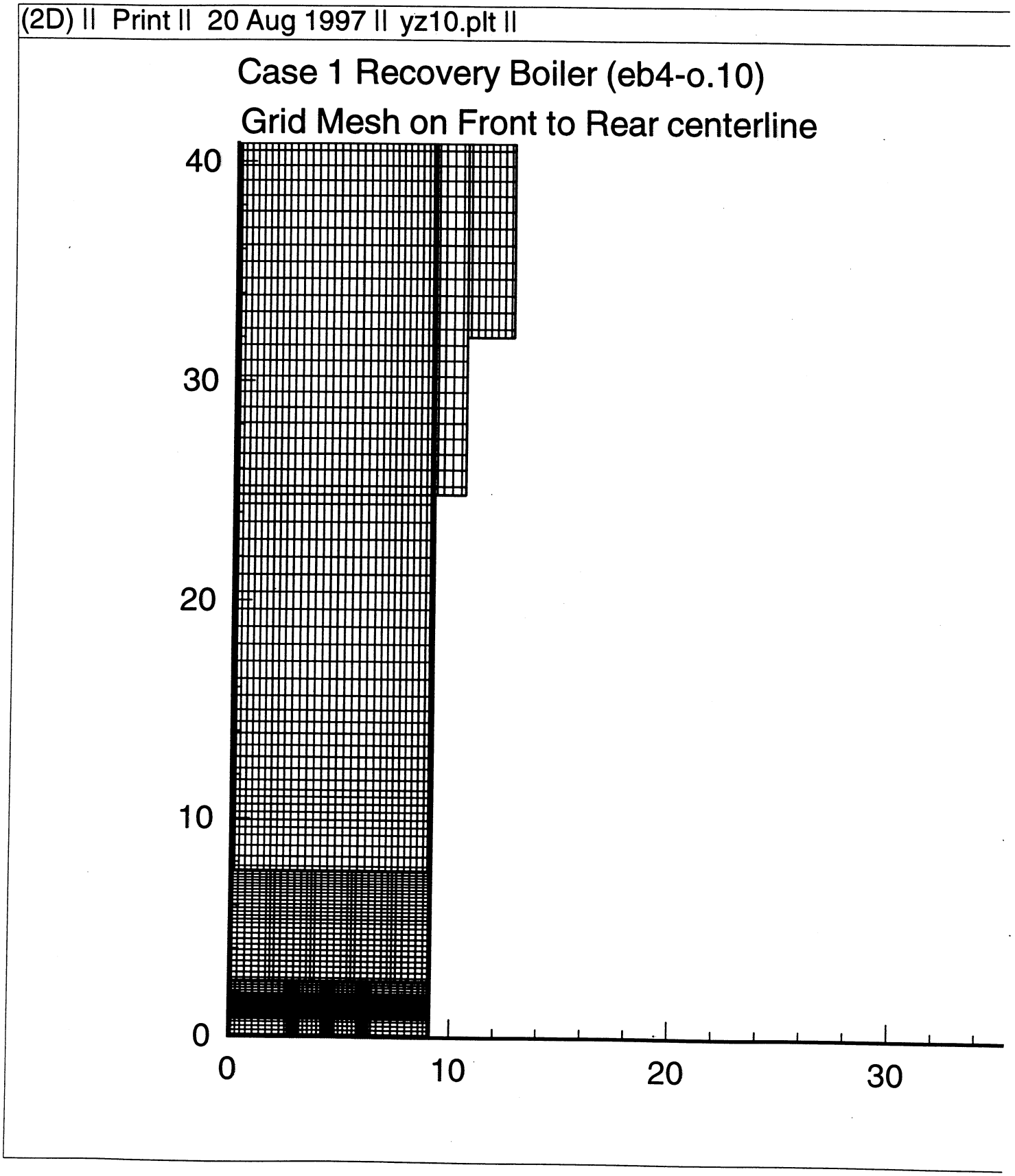

Figure 2. Grid for Case 1 Recovery Boiler Simulation.

Table 1. Air Inlet Conditions For Case 1 Recovery Boiler Model.

Air Level	No. of Ports	Port Area	Velocity	Total Air Flow	Temperature
		(m^2)	(m/s)	(kg/s)	(K)
Primary Air Ports	114	0.863	61.9	45.4	403
Gun Ports	16	0.372	9.1	4.0	298
Secondary Air Ports	12	0.619	69.1	38.0	397
Secondary Gas Ports	8	0.714	5.3	3.4	397

The boundary conditions are defined by default for the wall surfaces as zero velocity gradient. The wall temperatures are based on the default values in the UBC model. The temperature for the side walls of the boiler are set at 850 C. In the upper furnace the tube banks are assumed to have a uniform temperature of 407 C.

Spraying Conditions

The liquor to the boiler is fired from 16 nozzles, uniformly spaced, four on each wall. The nozzles used on this boiler are simply 1-1/4 inch pipe sections. Although it is difficult to determine the initial drop size and velocity of the spray, an estimate was made based on spray work performed using conventional nozzles. The initial velocity was estimated at 2.5 m/s and the mass median drop size is expected to be about 4.0 mm.

Additional testing was performed to study the effect of varying the inlet black liquor spray conditions. Mass median drop sizes of 2.0, 3.0 and 4.0 mm were tested. The initial drop velocity was also tested at 1.0, 2.5 and 4.0 m/s.

Simulation Results

Solution Procedure

This model was solved in a multi-staged procedure to achieve a converged solution. In the first stage only the flow field calculations were performed and the solver was run for 300 iterations. Next the combustion calculations were added along with the heat transfer equations and run during stage 2 for 300 iterations. In the third stage the radiation model calculations were added and performed simultaneously with the momentum, heat, and mass transfer calculations, which had been solved in the previous time step. Here again, 300 iterations were used. For each of the first three stages, the time step had an infinite length so the simulation was being solved as a steady state solution.

In the subsequent solutions the length of the time step was set to one second. Then the complete model simulation was performed for seven consecutive time steps, each for run for 300 iterations. By comparing the results of these individual time steps it became apparent that the solution was converging to a steady-state solution. The results presented below are from the final time step in this sequence. In addition one final time step was performed with an infinite time step (steady-state solution). The fact that this solution is virtually identical to the previous case confirms that the solution is at steady-state.

Flow Fields

The model calculates the flow pattern throughout the entire boiler and these results are graphed using Tecplot software as shown in the figures below. As is often found in recovery boiler simulations, there is a region of high upward velocity in the central region on the boiler. This high velocity core can be seen in the side view and the front view of the boiler (Figures 3 and 4). These contour plots represent the upward velocity on a single plane along the center-line of the boiler.

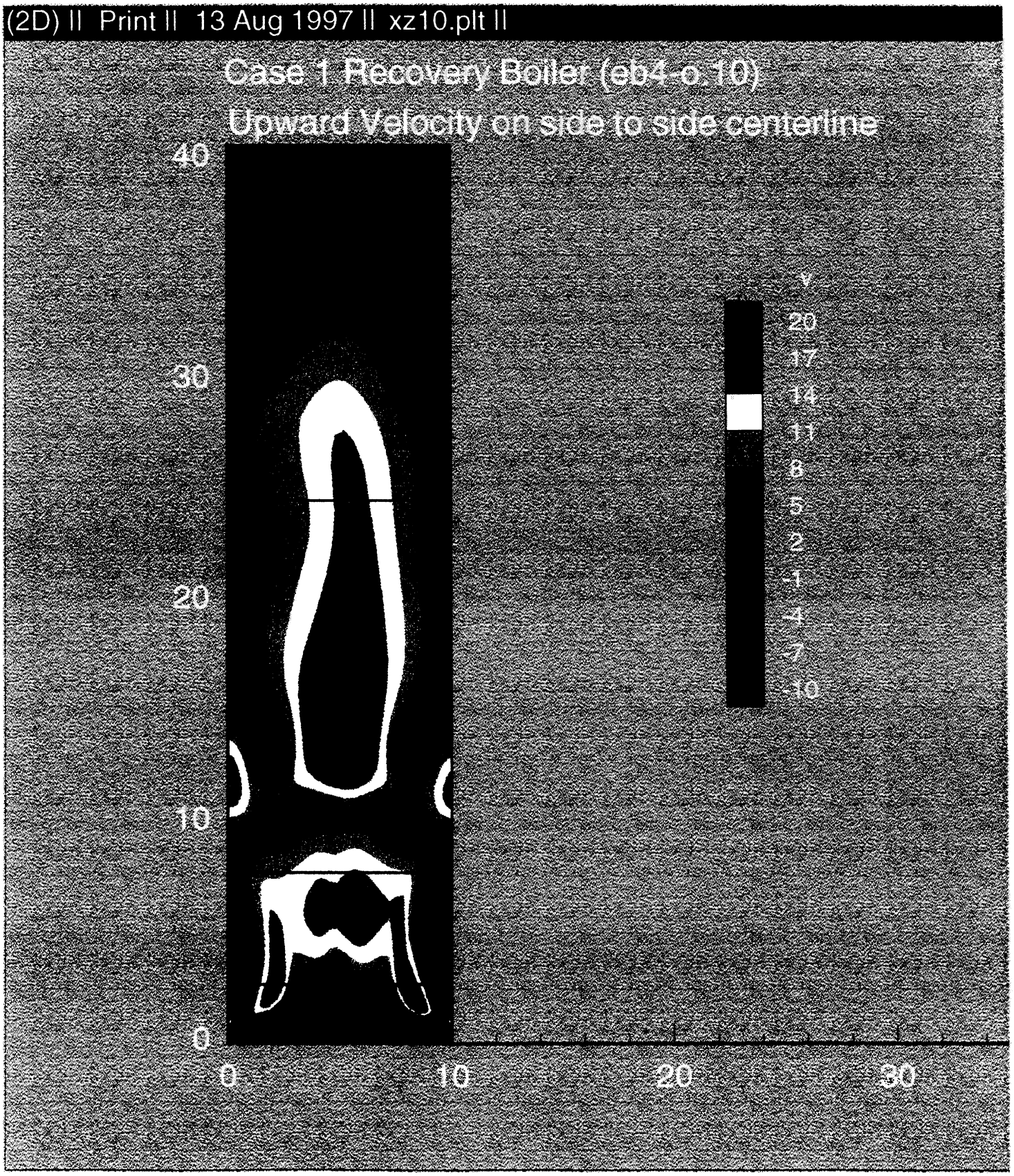

Figure 3. Upward Velocity on Front View of Case 1 Recovery Boiler.

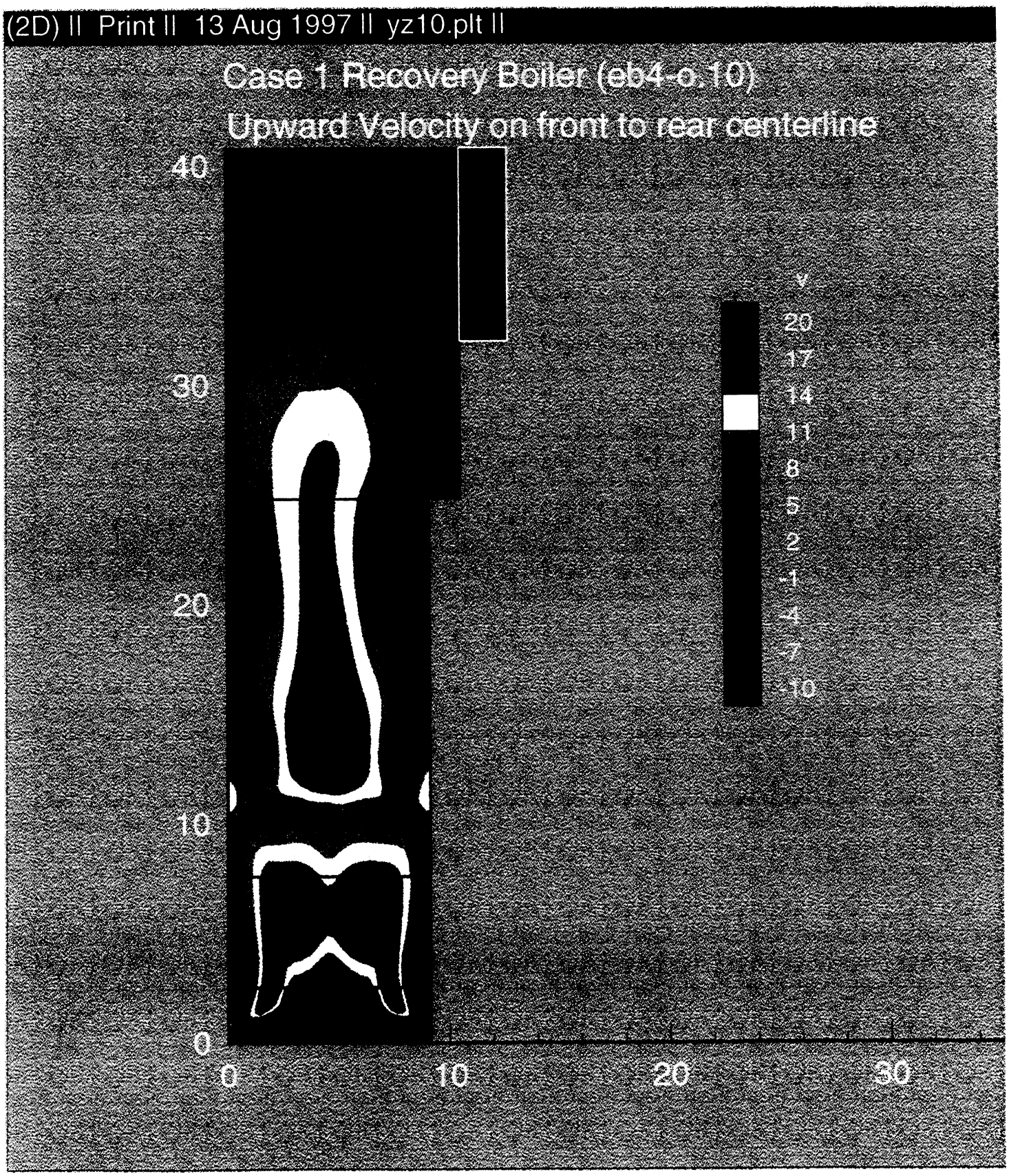

Figure 4. Upward Velocity on Side View of Case 1 Recovery Boiler.

In this simulation the central core begins to form above the char bed where the primary jets converge. The secondary air acts to break-up the core, but it reforms almost immediately and continues up into the superheater region of the boiler. This type central core is usually undesirable since it increases the amount of carryover and causes non uniformities in the heat transfer rate in the superheaters.

The boundaries of the graph represent the range of the grid structure, the bull-nose arch and the char bed are not shown explicitly but can be seen in the areas of zero upward velocity.

The upward velocity is also shown in plan view at two different elevations as shown in Figures 5 and 6 below. In Figure 5 the plan view shows the upward velocity at an elevation of 6.7 m above the floor of the boiler. This corresponds to the elevation of the black liquor gun ports. At this location the inlet flows from the primary air ports have been diverted upward after impinging on the char bed, and then merged together forming the central core.

The next figure (6) is the plan view at an elevation of 970 inches (24.6 m), which is just below the start of the bullnose arch. The orientation of the view is such that the bullnose is located at the top of the figure and the effect of the bullnose can be seen in the lower upward velocity at the top edge of the figure. Although the central core is temporarily broken up by the secondary air jets, it quickly reforms and continues into the upper furnace. Although it can not be seen in this figure, the secondary jets impart a counter-clockwise swirl to the overall flow (see Figure 9 below).

Temperature Profiles

The UBC model includes both momentum and energy balances so that it is capable of calculating the temperature throughout the boiler. The temperature predictions were plotted along the center-line of the boiler in a front view (Figure 7) and a side view (Figure 8). Both the orientation and the location of these slices are the same as used for the velocity profiles in Figures 3 and 4. Temperatures range from as high as 1500 C in the lower furnace above the char bed, to 500 C in the upper furnace. Overall the temperatures appear to be reasonable, but slightly higher than expected.

The shape of the temperature profiles is very similar to the velocity profiles shown above. There is a high temperature central core in the boiler due to the release of volatiles from the char bed and the cooling effect of the walls of the boiler. The average temperature at the bullnose plane is about 1100 C, which is somewhat higher than expected at this point. The high temperature core cools rapidly in the upper furnace due to the heat transfer surfaces. In fact, the cooling rate in the upper furnace seems to be over predicted in the model, so that the gas temperature at the boiler bank is lower than expected (500 to 600 C).

One final temperature profile is plotted in Figure 9. This plan view slice is at an elevation of 10.3 m which corresponds to the level of the secondary air ports. Although the variable plotted is temperature, the graph provides a good visual portrait of the jets leaving the secondary air ports. It can be seen from the figure that the flow is directed off the center-line of the boiler so that the flow is tangential to a circle in the middle of the boiler. This arrangement results in a counter-clockwise swirl (viewed from above) of the overall gas pattern.

Combustion Results

The UBC model includes the capability to model the behavior of the black liquor drops as they leave the gun port and to simulate the drying, pyrolysis, and char burning steps that the individual drops go through. In order to better understand the in-flight burning process in the recovery boiler model, several of the spraying parameters were varied to study the sensitivity of the model to these parameters.

The variables which were studied included the mass median drop diameter, the width of the drop size distribution, the initial velocity of the drops in the spray, the initial spray angle, and the width of the spray angle. The mass median drop diameter and the initial spray velocity were found to be the most important parameters.

Figure 5. Upward Velocity on Plan View at Gun Port Level (6.7 m).

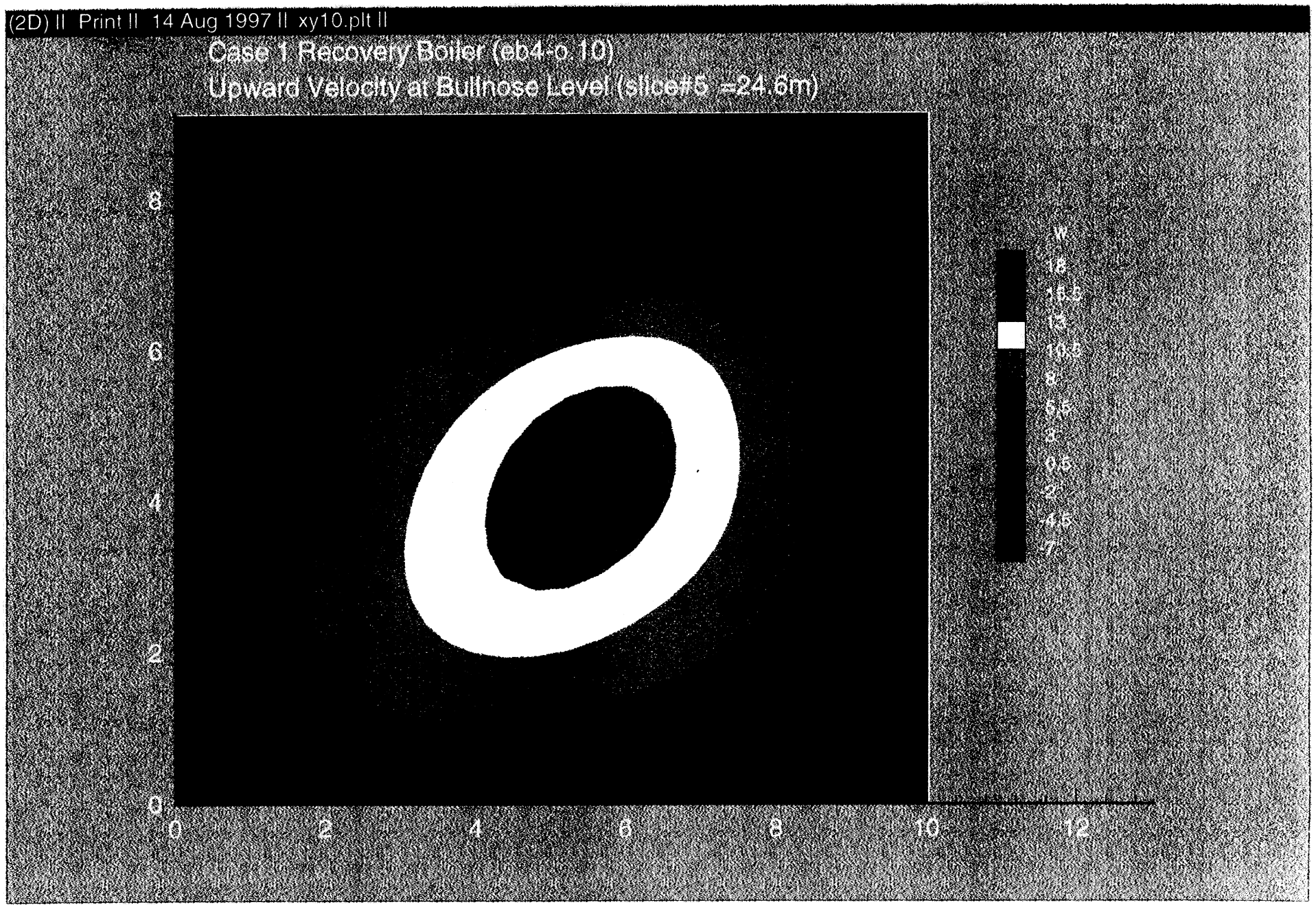

Figure 6. Upward Velocity on Plan View just below Bullnose (24.6 m).

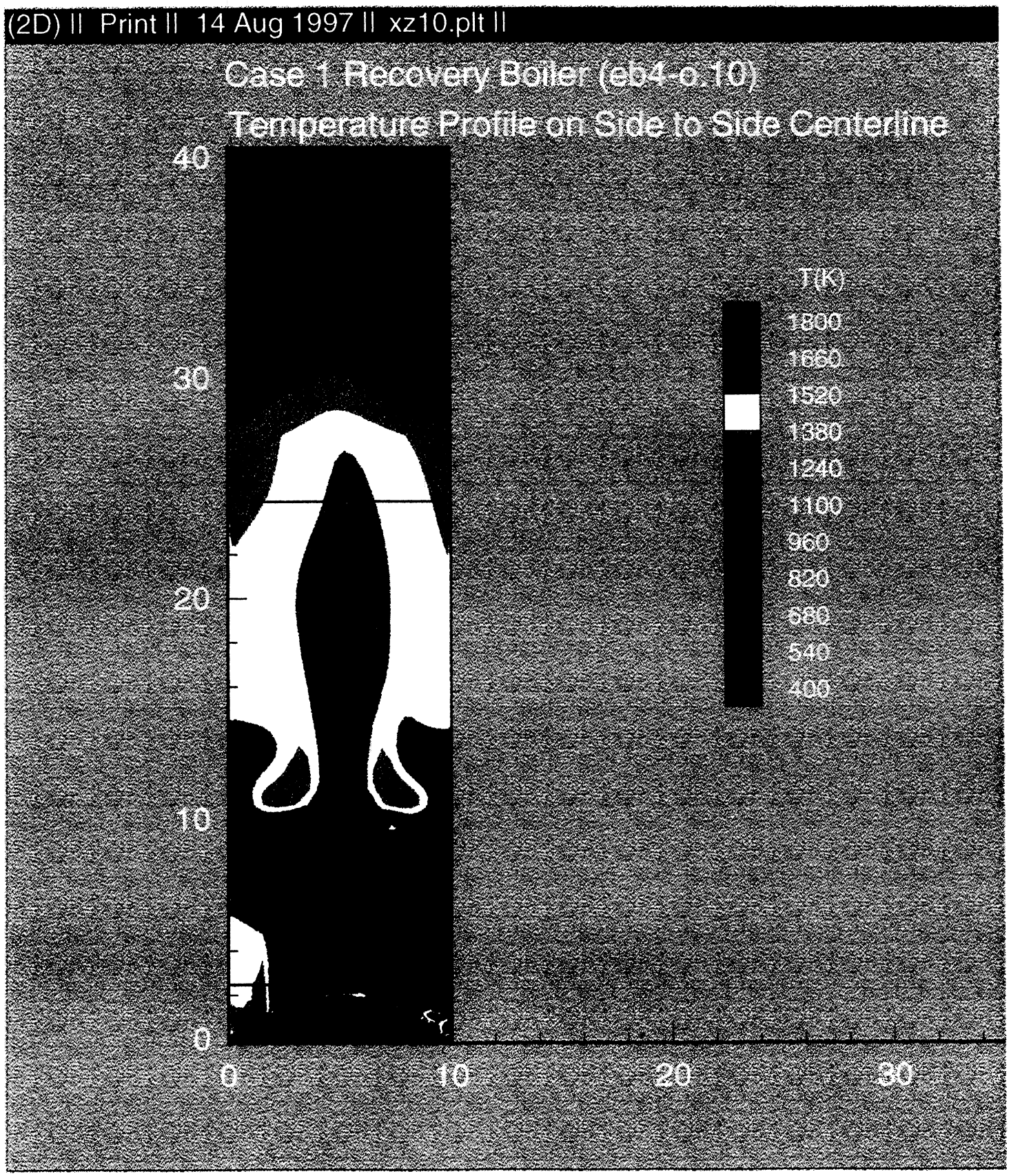

Figure 7. Temperature Profile on Front View of Case 1 Recovery Boiler.

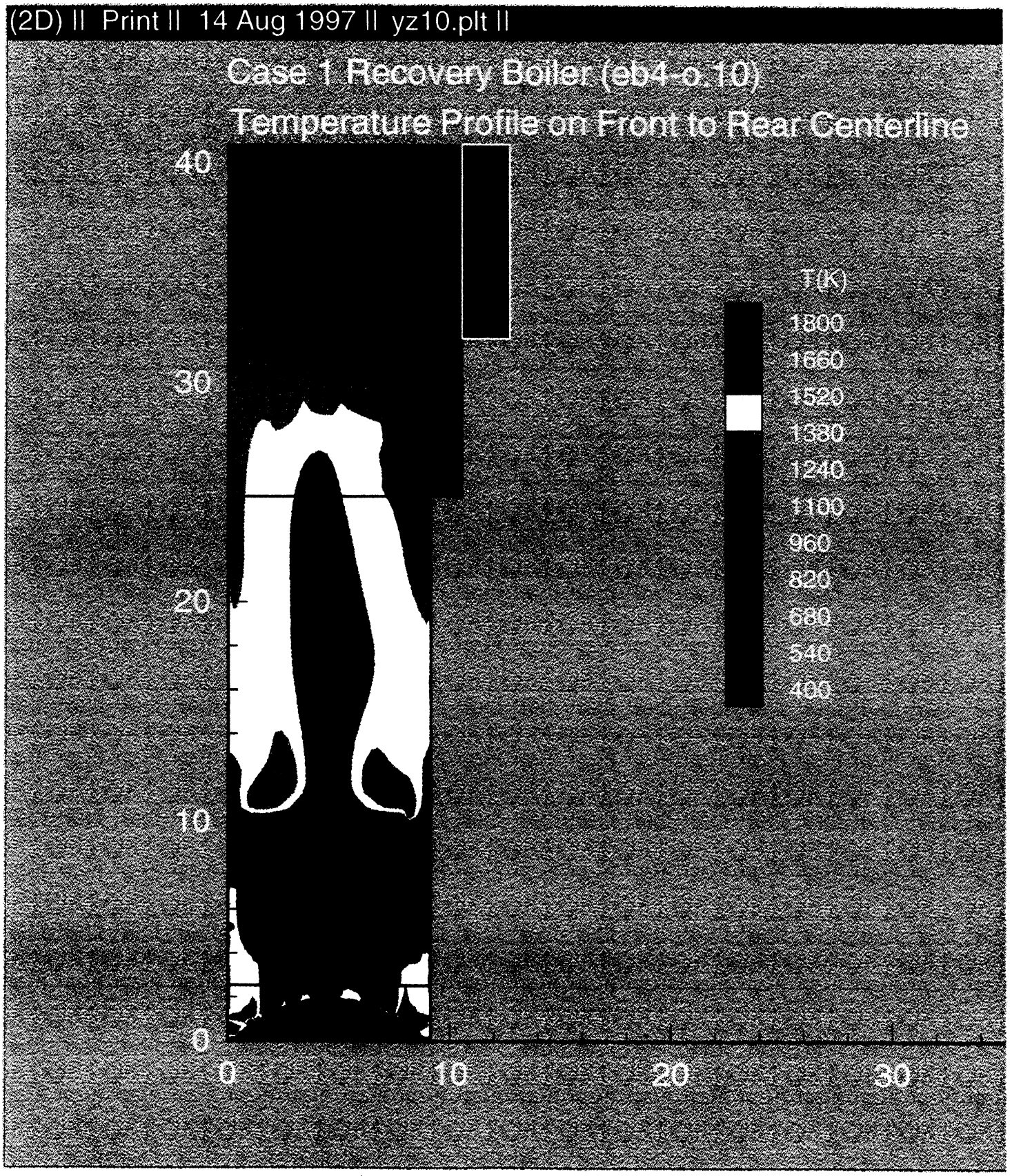

Figure 8. Temperature Profile on Side View of Case 1 Recovery Boiler.

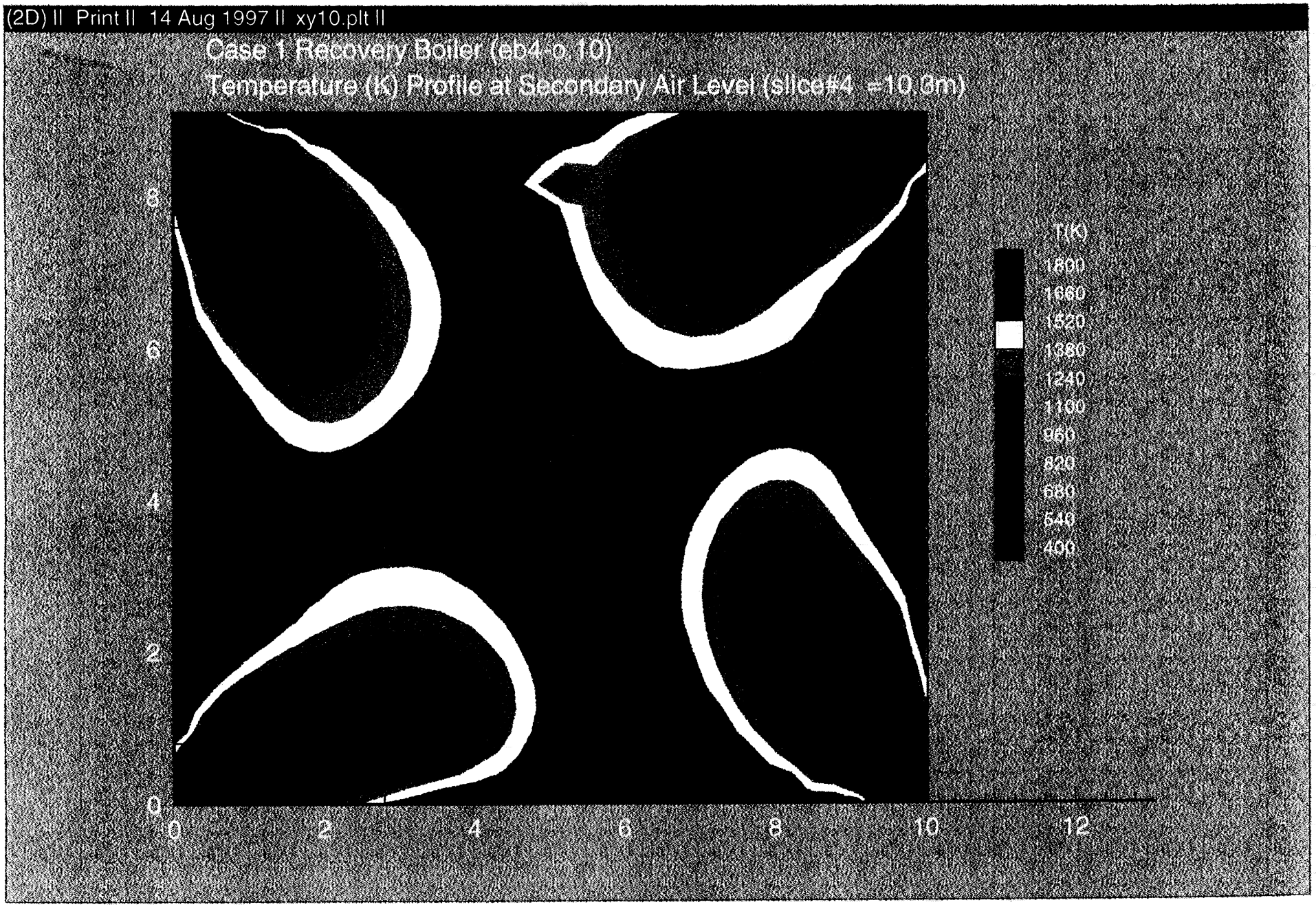

Figure 9. Temperature Profile on Plan View at Secondary Air Port Level (10.3 m).

The effect of the initial spray velocity can be seen most easily in a plot of the black liquor particles during the course of the burning. Shown below in Figures 10, 11 and 12 are the drop trajectories for velocities of 1.0, 2.5 and 4.0 m/s. For the low velocity case, the spray pattern drops down vertically and lands on the char bed very close to the wall. Increasing the velocity to 2.5 m/s results is the spray spreading farther into the reactor and the center of the spray pattern strikes the char bed about 2.5 m from the wall of the boiler. At the higher velocity (4 m/s) the spray pattern reaches almost to the center of the reactor before hitting the char bed.

The liquor in the model is composed of four general components; water, volatiles, char and smelt. The area of the boiler where these components has been released or consumed is also divided into four areas; in-flight, char bed, wall burning and carryover. The effect of drop diameter and inlet velocity on the distribution of these liquor components is shown below in Table 2. In this table the black liquor includes the initial water content (not on a dry solids basis), so most of the in-flight mass loss is due to evaporation of water.

Increasing the mass median drop size results in the less of the black liquor burning in-flight and more reaching the char bed. It also results in a reduction in the amount of black liquor reaching the walls of the boiler.

The initial drop velocity has a strong influence on where the black liquor is consumed. As the velocity increases more of the liquor burns in-flight and less is available to reach the char bed of the boiler. In addition the higher velocity means that more of the black liquor will eventually strike the walls of the boiler.

Table 2. Distribution of Black Liquor Components in the Recovery Boiler.

	Percent of Total Black Liquor				
Case	In-fight	Bed	Wall	Carry	Total
Effect of Drop Size at 2.5 m/s					
Small Dm (3.0 mm)	36.81	51.07	11.24	0.88	100.00
Medium Dm (4.0 mm)	28.61	63.71	7.16	0.51	100.00
Large Dm (5.0 mm)	23.17	71.95	4.56	0.32	100.00
Effect of Spray Velocity					
Low Velocity 1.0 m/s	23.07	74.26	2.39	0.28	100.00
Med Velocity 2.5 m/s	28.61	63.71	7.16	0.51	100.00
High Velocity 4.0 m/s	32.97	54.17	11.48	1.38	100.00

For all of the cases the amount of carryover predicted is low (Table 3). Only a relatively small number of drops reach beyond the bullnose into the upper furnace. For the base case (Dm = 4.0 mm, Vel = 2.5 m/s) the amount of carryover past the bullnose is 0.11 kg/s. This represents only 0.5% of the black liquor going into the furnace. At lower velocity the amount of carryover is reduced to 0.28% of the black liquor, and at higher velocity the carryover increases to 1.4% of the black liquor.

The mass median drop size also has an impact on the amount of carryover. As expected, reducing the drop size results in more carryover (0.88% of black liquor) and increasing the drop size results in lower levels of carryover (0.33% of black liquor).

Table 3. Carryover of Black Liquor into Upper Furnace.

	Spray Inlet			Carryover	
	Dm	Vel		Plane #1	
	(mm)	(m/s)		[kg/s],	%/BL
Effect of Drop Size at 2.5 m/s					
Small Dm (3.0 mm)	3.00	2.5		0.19	0.88%
Med Dm (4.0 mm)	4.00	2.5		0.11	0.51%
Large Dm (5.0 mm)	5.00	2.5		0.07	0.33%
Effect of Spray Velocity					
Low Velocity 1.0 m/s	4.00	1.0		0.06	0.28%
Med Velocity 2.5 m/s	4.00	2.5		0.11	0.51%
High Velocity 4.0 m/s	4.00	4.0		0.30	1.40%

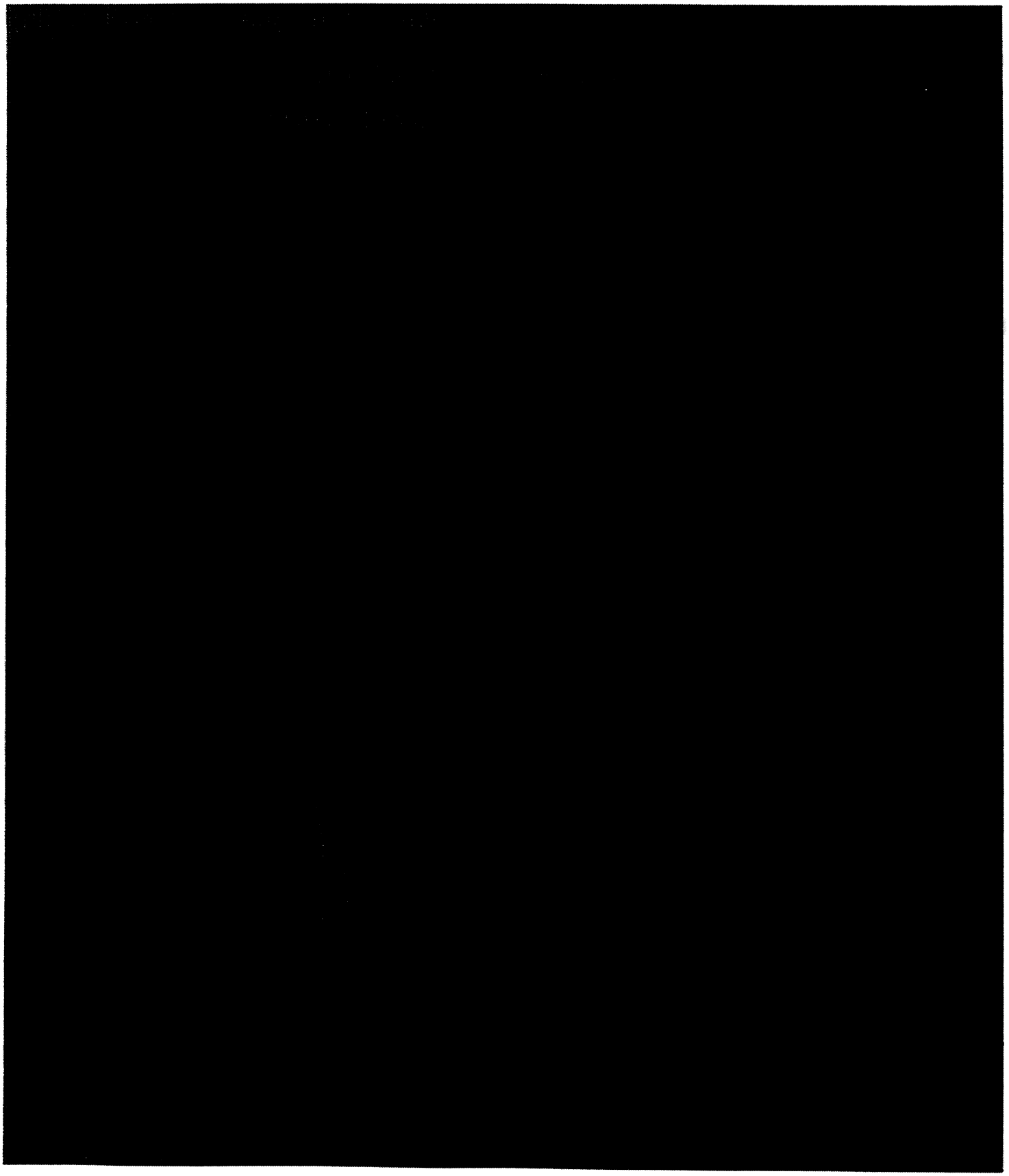

Figure 10. In-flight Black Liquor Trajectory (1.0 m/s initial velocity).

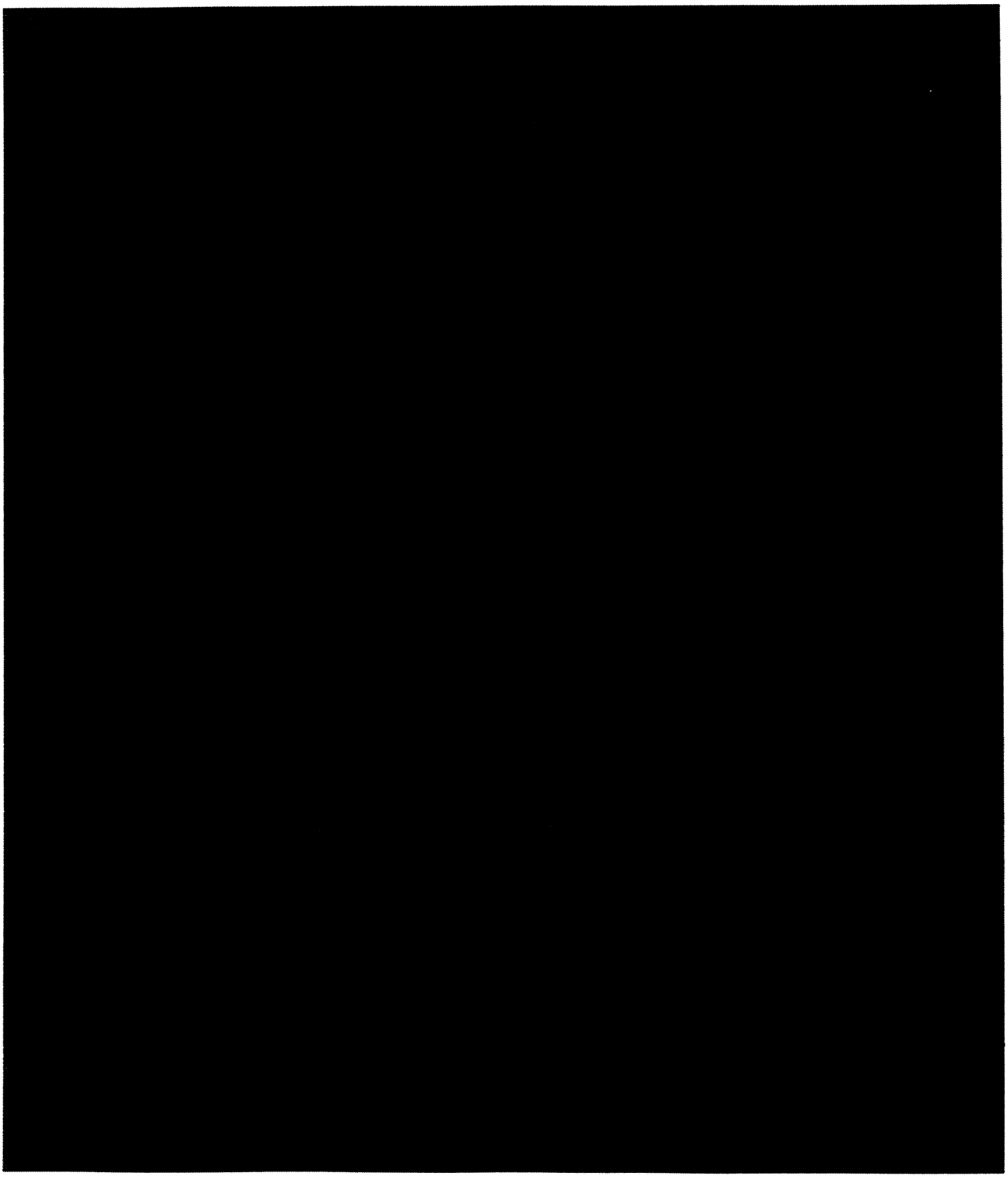

Figure 11. In-flight Black Liquor Trajectory (2.5 m/s initial velocity).

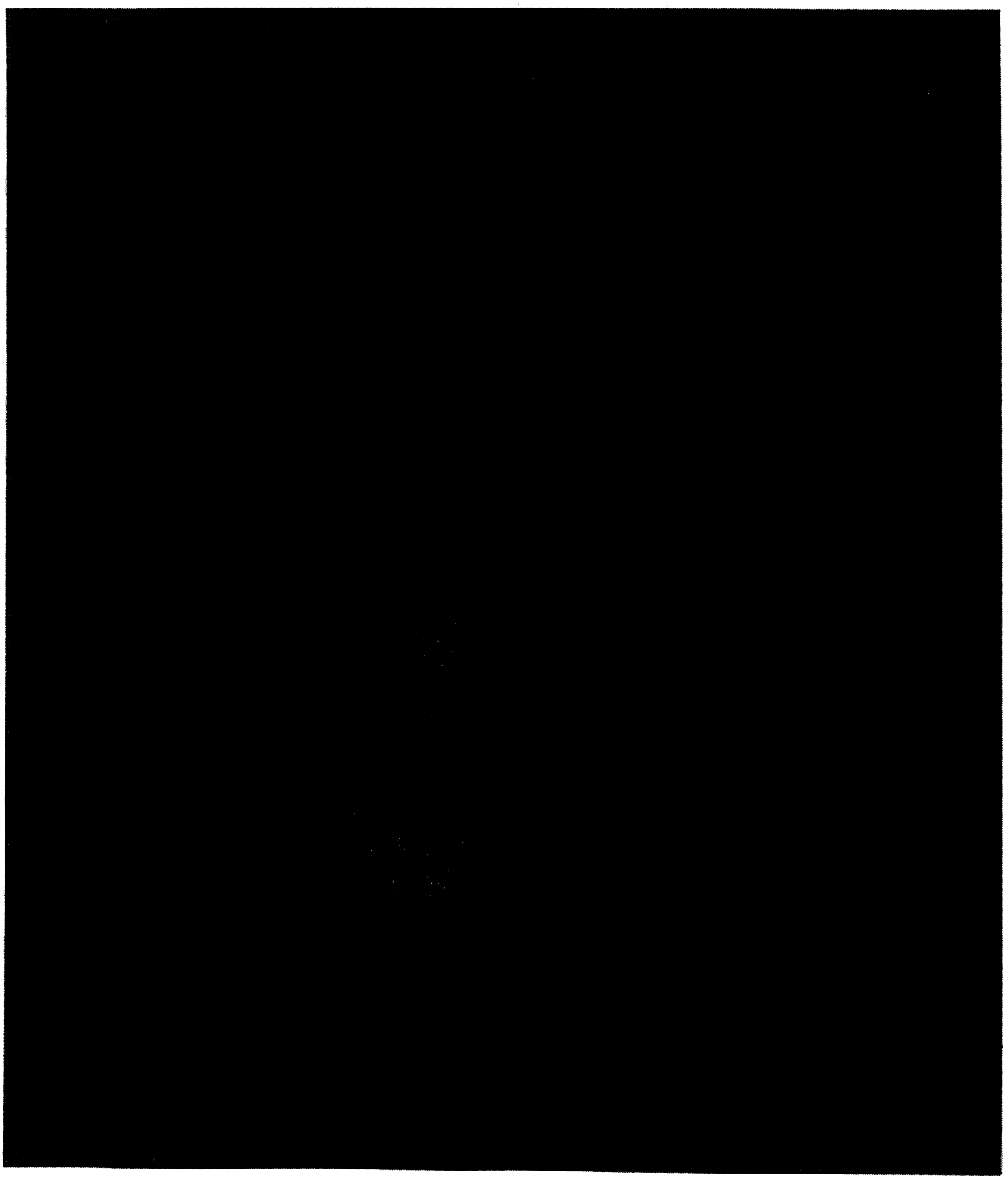

Figure 12. In-flight Black Liquor Trajectory (4.0 m/s initial velocity).

Comparison to Validation Data

As a joint effort between IPST and the University of Toronto, a set of data was collected at the Case 1 recovery boiler. This data was used in the setup of the model as described in the previous section. A limited amount of data was also available to use in verifying the results predicted by the model. The data which was collected during the mill trial is summarized in a separate report submitted to DOE (Data for Model Validation Summary Report by Grace et al.).

The first part of the data which was collected was required to setup the recovery boiler model. This includes the geometry of the boiler, the inlet conditions for the air flow (velocity and temperature), and the initial conditions for the black liquor sprays. The second part of the data collected had the potential to be used to verify the accuracy of the model predictions.

A large data set was collected on the temperature distribution of the char bed. However, in the current state of the recovery boiler model, the char bed temperature is an input variable which is not calculated by the model. Therefore this data set can not be used to validate the model. The remaining data which is usable for validation, consists of some gas temperatures measured in the upper furnace and videotaped images of the initial black liquor spray trajectories.

The comparison of the predicted gas temperature versus measured gas temperature is listed in the following table. The measured temperature is a line of sight reading of the gas temperature from an infrared pyrometer. The computed value is an average temperature from the model, across the width of the boiler at the same location.

The two sets of values are in reasonable agreement. The calculated gas temperature appears to be higher than expected at the bullnose arch, but on entering the heat transfer regions of the upper furnace it cools off rapidly and is lower than the measured temperature at the entrance to the boiler back. These results imply that the amount of heat transfer to the walls of the furnace cavity are lower in the model than in the actual furnace, and that the heat transfer to the superheater and generating banks is higher in the model than in the actual boiler. This is possibly due to the low default values for the tube temperatures in the upper furnace, and the inability of the model to account for the heat resistance of the tube fouling.

Table 4. Computed Gas Temperature versus Measured in the Upper Furnace.

Furnace Location	Measured Temperature (C)	Computed Temperature (C)
Near Bullnose (26 m elevation)	985	1065
Primary Superheater (36 m elevation)	714	722
Boiler Bank Inlet (36 m elevation)	595	545

During the mill trial a Babcock and Wilcox Char Bed Imaging Camera was used in an attempt to obtain additional information on the behavior inside the furnace. Due to the difficulty inherent in obtaining pictures in a fume filled furnace, very little could be seen with this camera. The most useful images are those of the black liquor spray leaving the nozzles. The images were obtained from the left hand gun port on the left (west) wall of the boiler. From this position two of the spray patterns can be seen on the adjacent rear (north) wall of the boiler. These are the two nozzles nearest to the left wall.

The video images were transferred from video tape by a frame grabber, and analyzed with a PC based image analysis system. Although it was relatively easy to see the two spray jets on a video monitor, it was difficult to obtain a clear image in a digital format. The best result was obtained by capturing thirty-two video images and averaging them and storing it in a TIF format. This image is shown below in Figure 13. The nearest of the two jets is clearly visible traveling from the upper left toward the lower right. The second spray jet can be seen faintly above the first nozzle The large dark section in the lower center of the image is the spray nozzle in the port where the camera is located.

In order to compare the results of the model predictions to experimental data, a second image of the spray pattern based on the model was generated (Figure 14). The trajectories are shown from the same view-point as the video image, although with a slightly different magnification. The trajectories as shown are quite similar to those obtained from the video camera. Based on these trajectories it was apparent that the initial drop velocity is much higher than would be expected based on the flow-rate and nozzle diameter (1.0 m/s). This increased velocity is due to the flashing of black liquor at the nozzle. As the hot liquor encounters lower pressures, steam is generated which increases the velocity leaving the nozzle. The velocity used in the model image is 5.0 m/s, so it appears that the actual velocity is at least this fast and possible slightly higher.

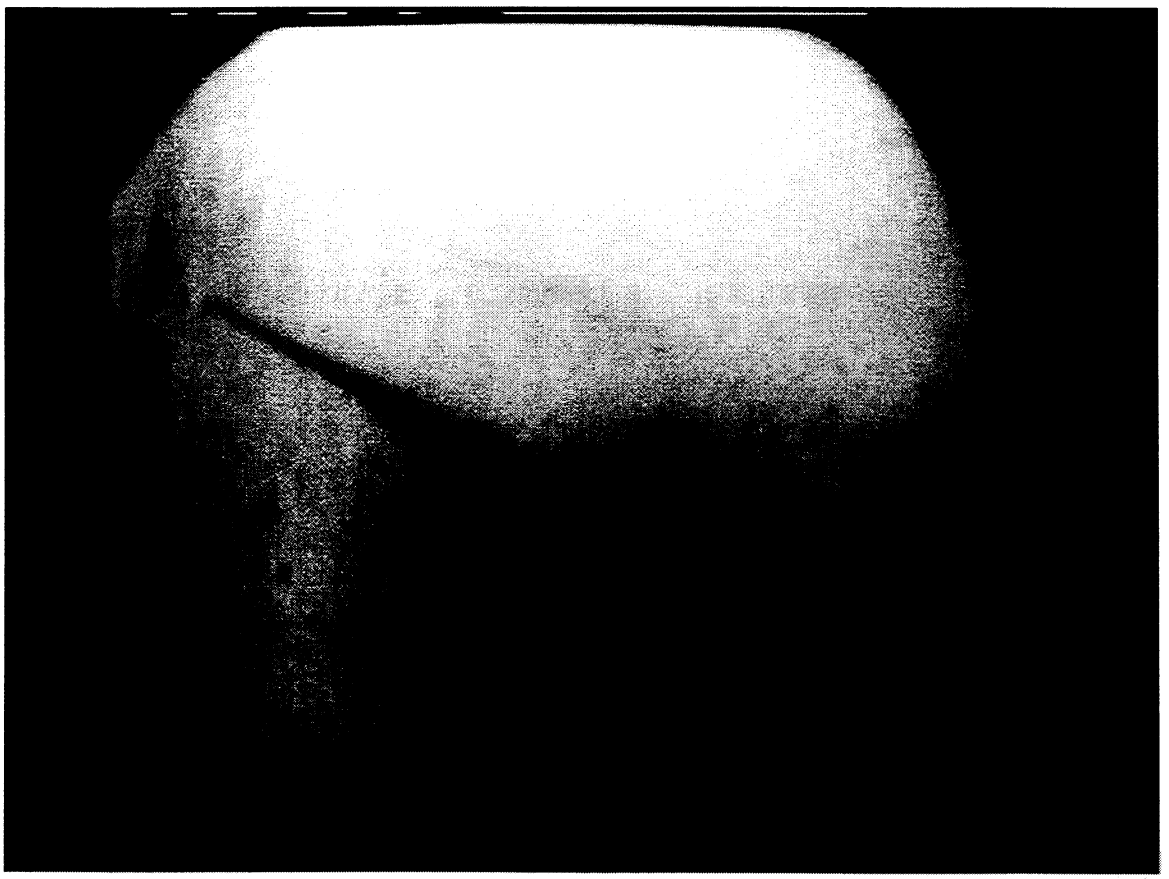

Figure 13. In-flight Black Liquor Trajectory from Video.

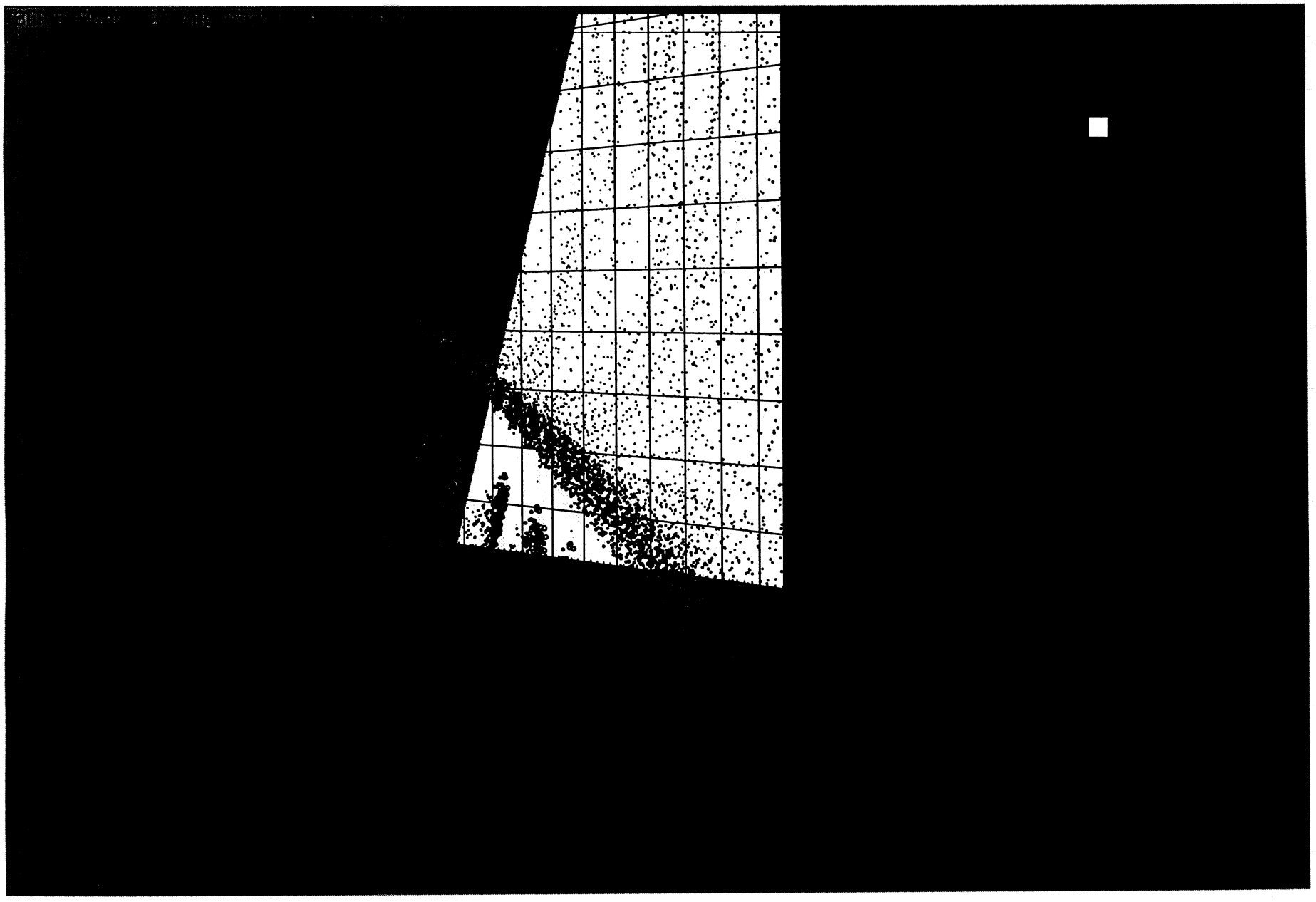

Figure 14 In-flight Black Liquor Trajectory from Model (5.0 m/s initial velocity).

Case 2

In July of 1996 a second set of physical measurements were made at another recovery boiler for use in validating the predictions obtained from recovery boiler models. As in the first case, a model simulation was set-up and solved using the computational fluid dynamics (CFD) model which was developed at the University of British Columbia. The simulation was performed as a cooperative effort between IPST and UBC.

During the test period at the mill, the recovery boiler operating conditions were varied to study the impact of the changing the inlet air distribution, the amount of excess air, the overall boiler loading, and the black liquor firing temperature. Eighteen different control conditions were tested and the results of these measurements are included as a separate report to DOE (Data for Model Validation Summary Report by Grace et al.). Due to the difficulty in obtaining a converged solution with the recovery boiler model, only a single test condition was simulated using the UBC model.

Model Setup

Geometry and Grid

This unit is a relatively small recovery boiler with overall dimensions of 254 inches (6.45 m) from front to rear, 266 inches (6.76 m) from side to side, and an overall height of 1138 inches (28.9 m) as shown in Figure 15. The recovery boiler is an older unit which had been retrofitted by Tampella within the last ten years. It has a rated capacity of 1.5×10^6 lb./day of black liquor solids and uses a three level air system. The arrangement of the air ports and other openings to the boiler are described in this section.

The primary air enters on all four sides. The primary ports are located at a centerline elevation of 42 inches (1.07 m) above the floor of the boiler. There are 15 ports on each of the four walls, for a total of 60 primary air ports. Horizontally the ports are spaced 15 inches from centerline to centerline. For this model each of the ports was individually defined. The ports in the model are defined as rectangular openings, three inches wide and 6.2 inches high. The actual ports are roughly diamond shaped and are slightly taller and narrower, but with the same area (of 18.6 in^2 per port).

The secondary air ports are located on the left and right sides of the furnace, at an elevation of 91 inches. The boiler has a total of ten secondary air ports - five on the right wall and five on the left wall. Both the primary and secondary ports are symmetric with those on the opposite wall. The arrangement of these ports is shown below in Figure 16. The model ports have dimensions of 6 inches wide and 9.3 inches high for at port area of 56 in^2, closely matching the actual port size. The boiler also has two large starter burners on the left wall and two more on the right wall. During normal operation of the boiler these ports are not used, so these were not included in the model.

The tertiary ports are located at an elevation of 318 inches. There are three ports on the front wall and four ports on the rear wall in an interlaced configuration. In general, this mill uses low tertiary velocities. The model ports have dimensions of 5 inches wide by 8 inches high. The port arrangement is shown in Figure 17 below. In addition, Table 5 contains the critical dimensions for all of these ports.

The black liquor gun ports are arranged at an elevation of 201 inches. There are three gun ports on both the right and left wall on a 39 inch centerline spacing. The current firing practice at the mill is to use only the two outside gun ports on each wall, so the center port on each wall is closed off. The gun ports are included in the grid arrangement for this model. There are also 3 smelt spouts on the front wall of the furnace at an elevation of 12 inches.

The model was setup to include the upper furnace heat transfer regions including the superheaters and up to the center-line of the generating bank. The grid is separated into five different segments to allow for a finer grid in the lower furnace to accurately model the air ports and a coarser grid in upper furnace to reduce the computational load on the computer. The grid structure is shown in Figure 18.

Table 5. Air Port Arrangement

Air Level	Side	Elevation (in)	Number of Ports	Horizontal Spacing (in)	Port height (in)	Port width (in)	Individual Port area (in^2)	Total Port area (in^2)
Smelt Spouts								
	Front	12	3	48	6.5	4	18.1	54.4
Primary Ports								
	Left	42	15	15	9	4	18.6	279.0
	Right	42	15	15	9	4	18.6	279.0
	Front	42	15	15	9	4	18.6	279.0
	Rear	42	15	15	9	4	18.6	279.0
	All	42	60	15	9	4	18.6	1116.0
Secondary Ports								
	Left	91	5	30/60	17	6	55.8	279.0
	Right	91	5	30/60	17	6	55.8	279.0
	All	91	10	30/60	17	6	55.8	558.0
Gun Ports								
	Left	201	3	39	8	5	40.0	120.0
	Right	201	3	39	8	5	40.0	120.0
	All	201	6	39	8	5	40.0	240.0
Tertiary Ports								
	Front	318	3	39	13	6	43.4	130.2
	Rear	318	4	39	13	6	43.4	173.6
	All	318	7	39	13	6	43.4	303.8

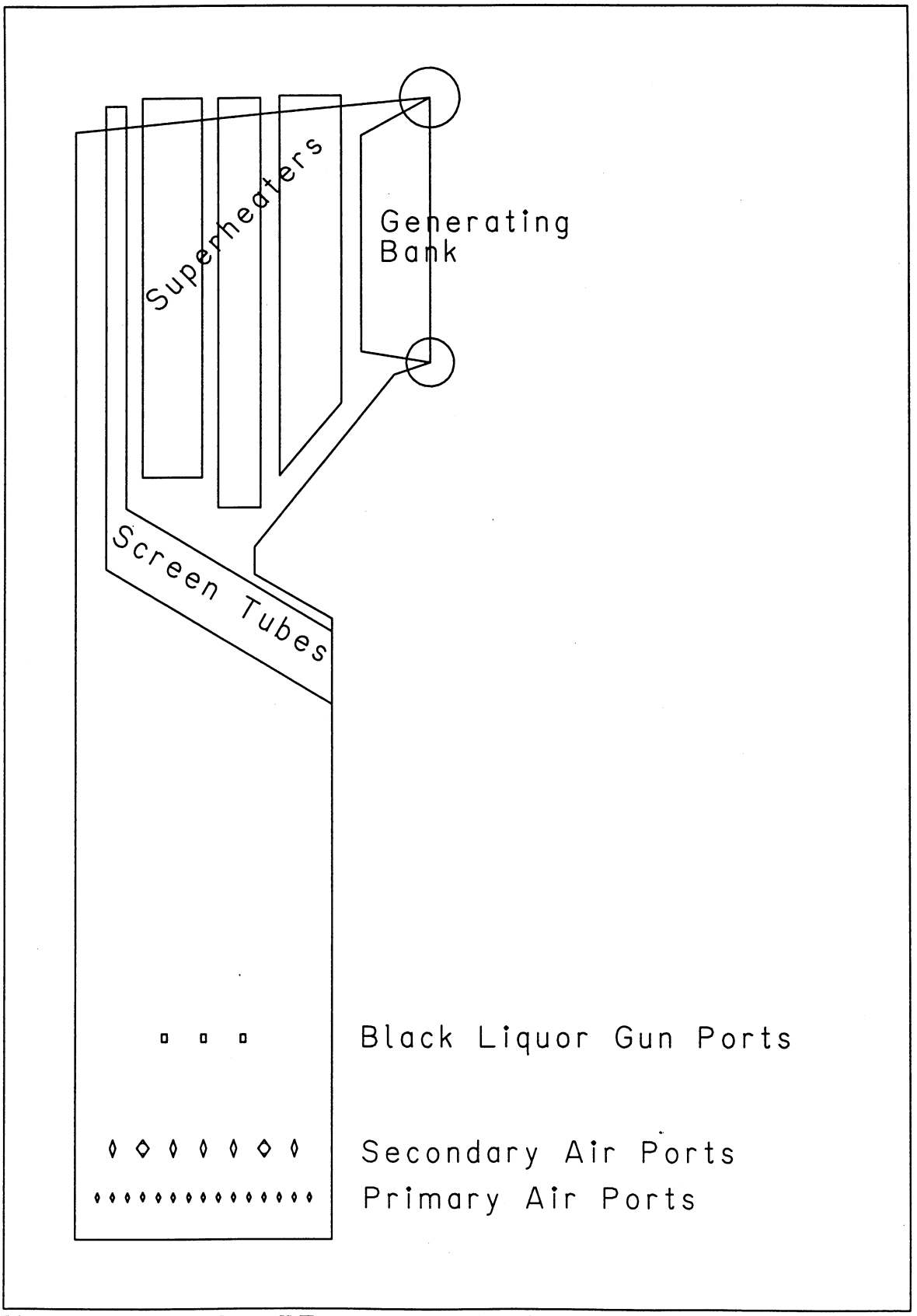

Figure 15. Case 2 - Overall Furnace Right Elevation.

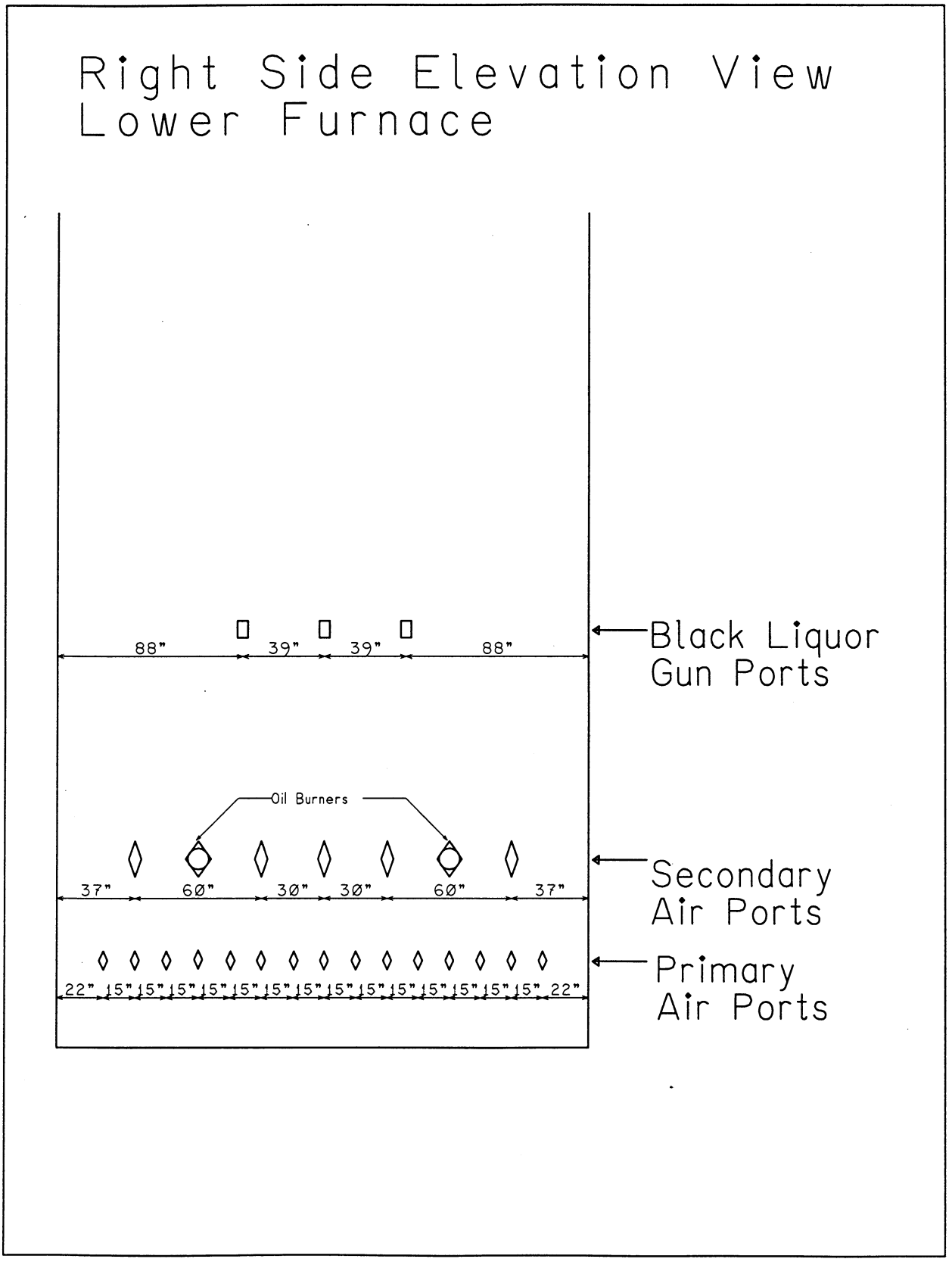

Figure 16. Case 2 - Air Port Arrangement - Right Elevation Lower Furnace.

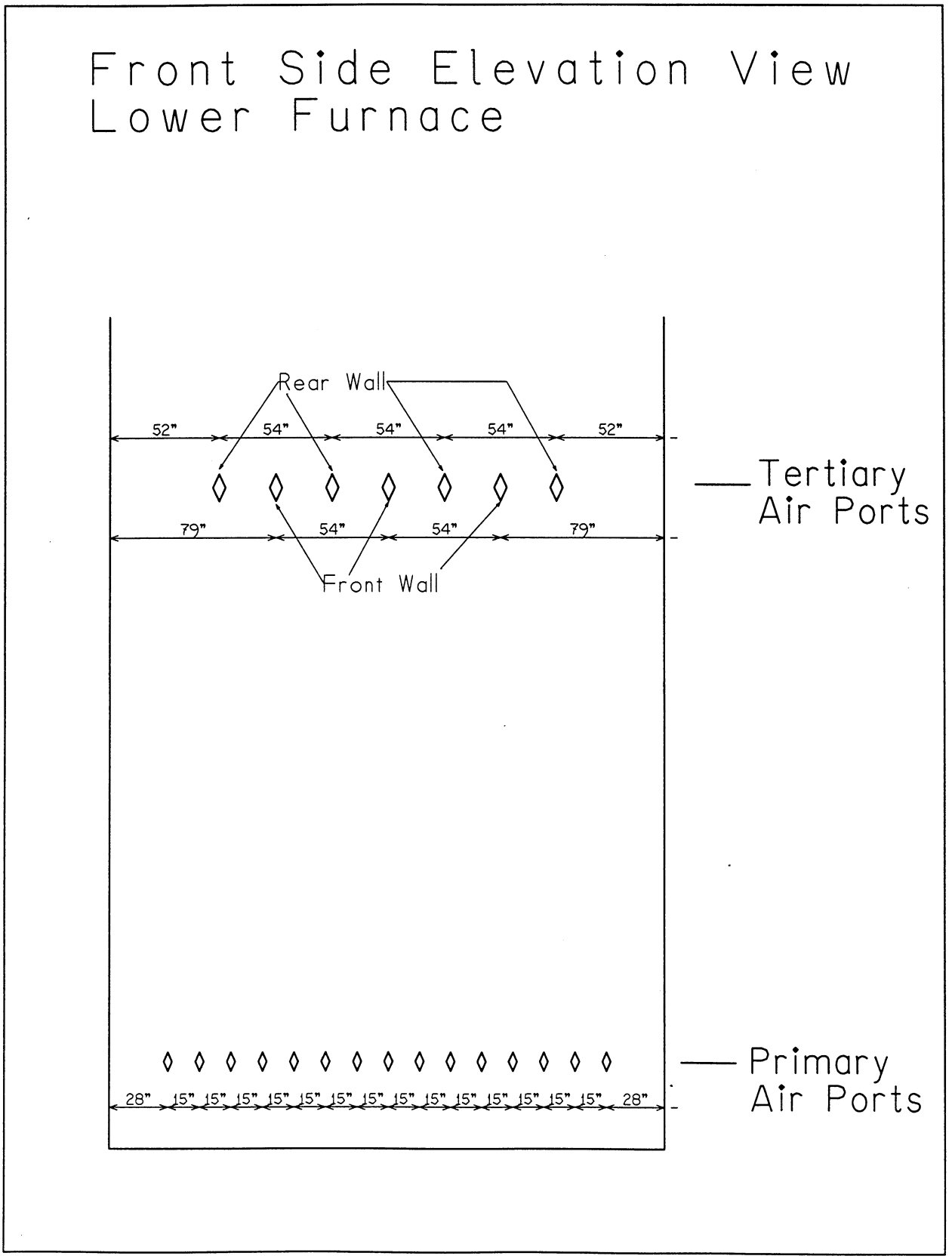

Figure 17. Case 2 - Air Port Arrangement - Front Elevation Lower Furnace.

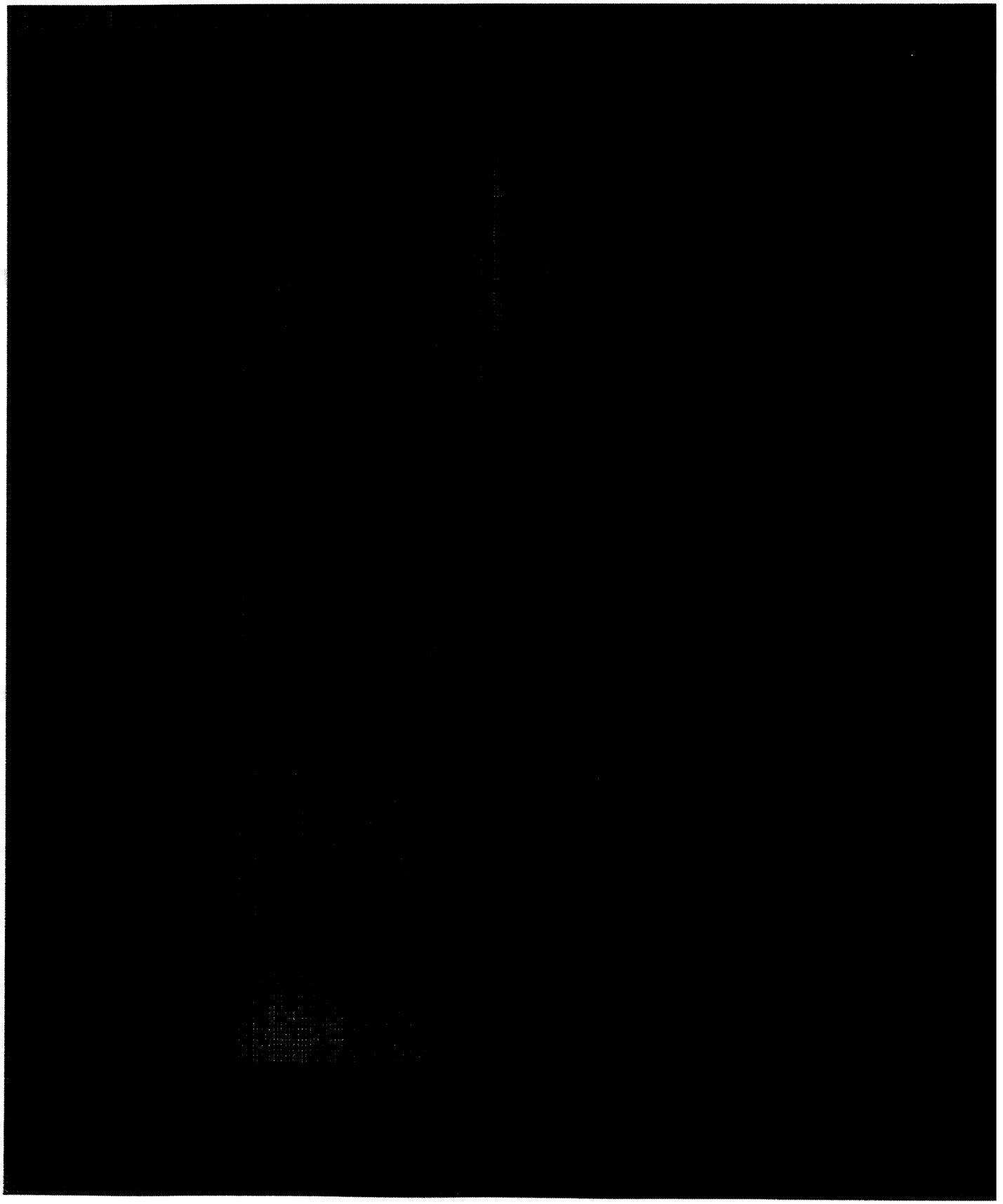

Figure 18. Case 2 - Grid Layout for Recovery Boiler Furnace Model.

Inlet Conditions

The model was setup to match the typical operating conditions for this recovery boiler. The air inlet velocities at all of the ports are listed below in Table 6. The inlet jet velocities were calculated based on the mass flow rates reported by the mill during the initial testing (when the boiler was operating at typical conditions). From the measured flow rates and dimensions of each individual port, a velocity value can be calculated for the flow through each port. A summary of these values is shown below in Table 6. At the primary level, the inlet velocity is a constant value of 19.9 m/s. For the secondary jets a calculated velocity was 44.0 m/s. At the black liquor gun ports an air leakage rate of 5% of the inlet primary, secondary and tertiary air flow was assumed, which gave an inlet velocity of 8.0 m/s. At the tertiary level the inlet velocity is 15.7 m/s.

The air flow to the primary and secondary ports is preheated to a temperature of 150 C. At the gun ports and the tertiary levels the air is not heated and was at an ambient temperatures of about 30 C. A turbulence intensity of 10% was assumed for all of the air inlet ports in the model definition.

Table 6. Air Inlet Conditions For Case 2 Recovery Boiler Model.

							Turbulence
Air Level	Flow	Flow	No. of	Area	Temp	Vel	Intensity
	(kg/s)	(%)	Ports	(m^2)	(K)	(m/sec)	(%)
Primary	11.97	39.6%	60	0.72	423	19.89	10.0%
Secondary	13.24	43.8%	10	0.36	423	44.00	10.0%
Gun Ports	1.44	4.8%	6	0.144	303	8.00	10.0%
Tertiary	3.60	11.9%	7	0.196	303	15.73	10.0%
Total	30.24	100.0%	83	1.42			

Boundary Conditions

The boundary conditions are defined by default for the wall surfaces as zero velocity gradient. The wall temperatures are based on the default values in the UBC model. The temperature for the side wall of the boiler are set at 850 C. In the upper furnace the superheater tube banks are assumed to have a uniform temperature of 417 C, and the temperature for the generating tube banks and screen tubes was set at 327 C.

Spraying Conditions

Another crucial parameter in the application of recovery boiler simulations is the black liquor firing conditions. This mill uses four Tampella nozzles (24 mm diameter), two on the left and two on the right wall. Information on the firing conditions is listed below in Table 7. The flow-rate is "as-fired", measured after the salt-cake mix tank. The solids content from the mill control system was 68.6, the liquor temperature and the nozzle pressure are also listed.

Based on previous work performed at IPST, an estimated mean drop diameter was calculated. A drop size of 3.30 mm was calculated from a correlation which depends on the nozzle velocity (computed from the flow-

rate and nozzle diameter) and the black liquor viscosity. Because no data was available on the liquor viscosity at the firing solids and temperature, an estimate was made using a correlation for a typical black liquor. Due to these unknown factors, the estimated mean drop diameter may not be very accurate.

A second calculation was also performed to estimate the initial velocity of the drops leaving the nozzle. Because this value is less strongly dependent on the estimated viscosity, the predicted initial drop velocity of 5.7 m/s should be reasonably accurate.

Table 7. Black Liquor Firing Conditions For Case 2 Recovery Boiler Model.

	Nozzle	Nozzle	No. of	Mill	Mill	Mill	Estimated	Estimated
Run #	Type	Diameter	Nozzles	Solids	Temp	Flow	Dm-	Velocity
		(mm)		(%)	(C)	(gpm)	(mm)	(m/sec)
1a	Tampella	24	4	68.8	125.7	119.7	3.30	5.72

Simulation Results

Solution Procedure

This model was solved in a multi-stage procedure to achieve a converged solution. It was found that this model was somewhat unstable and tended to diverge, probably due to the arrangement of the directly opposed jets at the secondary air level. With the high initial velocity at these secondary ports the jets tend to impinge on the jet from the other side of the boiler, resulting in an unstable flow pattern. However, by using a multi-stage procedure, with relatively small incremental changes in the model, it was possible to get the simulation to converge to a steady-state solution.

Initially a simple model is used and then additional components of increasing complexity are added. In the first stage only the flow field calculations were performed and the solver was run for 2000 iterations in a steady-state mode. Next the combustion calculations were added along with the heat transfer equations and run during stage 2 for 1000 iterations, again as a steady-state model. In between each of the stages, the spray model is run to describe the behavior of the black liquor drops. In the third stage the same model was run for another 1000 iterations.

In the next stages the model is run as a transient (rather than steady-state) model with a time step of 1.0 seconds. This is repeated four times (each 1000 iterations) in stages 4 through 7. Next the radiation model calculations were added and performed simultaneously with the momentum, heat and mass transfer calculations which had been solved in the previous stage. Once again, 1000 iterations were used. As before, the spray model is run in between the time steps. Then the complete model simulation was performed for ten consecutive one second time steps, each run for 1000 iterations.

By comparing the results of these individual time steps it became apparent that the solution was converging to a steady-state solution. The flow settles to a steady state with little variations between successive time steps. The results presented below are from the final time step in this sequence. The steady flow field appears to be realistic and the flow has a fairly symmetric up-flow core.

Flow Fields

The model calculates the flow pattern throughout the entire boiler and these results are graphed using Tecplot software as shown in the figures below. A common feature found in the flow fields of recovery boiler simulations, is a region of high upward velocity in the center of the boiler. In many cases this high velocity core may persist into the upper furnace, with the potential for carryover and high temperature regions continuing into the super-heater. Velocity and temperature variations, resulting in non-uniform heat transfer rates in the upper furnace, are generally undesirable in a well-designed boiler. In this model a high velocity core is formed due to the secondary air jets.

This boiler has five secondary ports on both the left and right sides. The port arrangement is symmetric along the centerline of the boiler, so that the ports on the left wall are directly opposed to those on the right wall. Because of the high initial velocity of the secondary jets (44.0 m/s) and the small size of the boiler (6.76 m), the jets persist until they impinge on those from the other side of the boiler. The impact of the jets meeting creates a high turbulence zone and a then a strong upward flow. This can be seen below in Figure 19, where the velocity vectors are shown in a plan view at the secondary elevation.

The high velocity upward core exists in a region along the centerline, extending from front wall to the rear wall. This can be seen in Figure 20, showing the upward velocity contours plotted in a slice along the centerline of the boiler. The highest upward velocities occur in the lower part of the furnace, above the secondary air level and below the tertiary air level. The tertiary velocities are quite low in this boiler (15.7 m/s) and are not very effective in breaking up the central core. In addition the arrangement of the tertiary ports on the front and rear walls means that most of the tertiary jets do not directly impinge on the central core. It appears that most of the reduction in the velocity of the central core is due to the diffusion of the central core outwards.

From side to side, the high velocity core is relatively narrow, only about 2.0 m wide (Figure 21). As seen before, the highest upward velocities (>10 m/s) exist below the tertiary level. Above this the velocity is lower (5-8 m/s) but a distinct upward velocity core still exists, and continues into the superheater. Above the bullnose the high velocity core drifts off of the centerline and slightly toward the left side of the boiler. There is no apparent physical reason why the core should move off center and this may be an artifact of the model.

The upward velocity contours are shown in plan view for the slice at the elevation of the gun ports (Z=5.11 m) in Figure 22. The narrow ridge of upward flowing gas is obvious along the centerline of the boiler. It is also apparent that there are down-flow regions near the left and right sides of the boiler. These down-flow regions are part of a large re-circulation zone associated with the high velocity core. A small part of the upward flow splits off and travels downward along the walls until it reaches the secondary air jets where it is re-entrained in the upward flow pattern.

This high velocity core pattern passes the tertiary jets relatively unchanged and continues up to the bullnose arch. At this point the bullnose arch reduces the width of the boiler and the shape of the high velocity core is flattened out. This is seen in the upward velocity contour plot at the bullnose elevation in Figure 23. The gas velocities along the centerline of the boiler are much higher than those near the side walls (5 to 8 m/s vs. 2 to 4 m/s). The bull-nose arch is not show explicitly but can be seen in the areas of zero upward velocity.

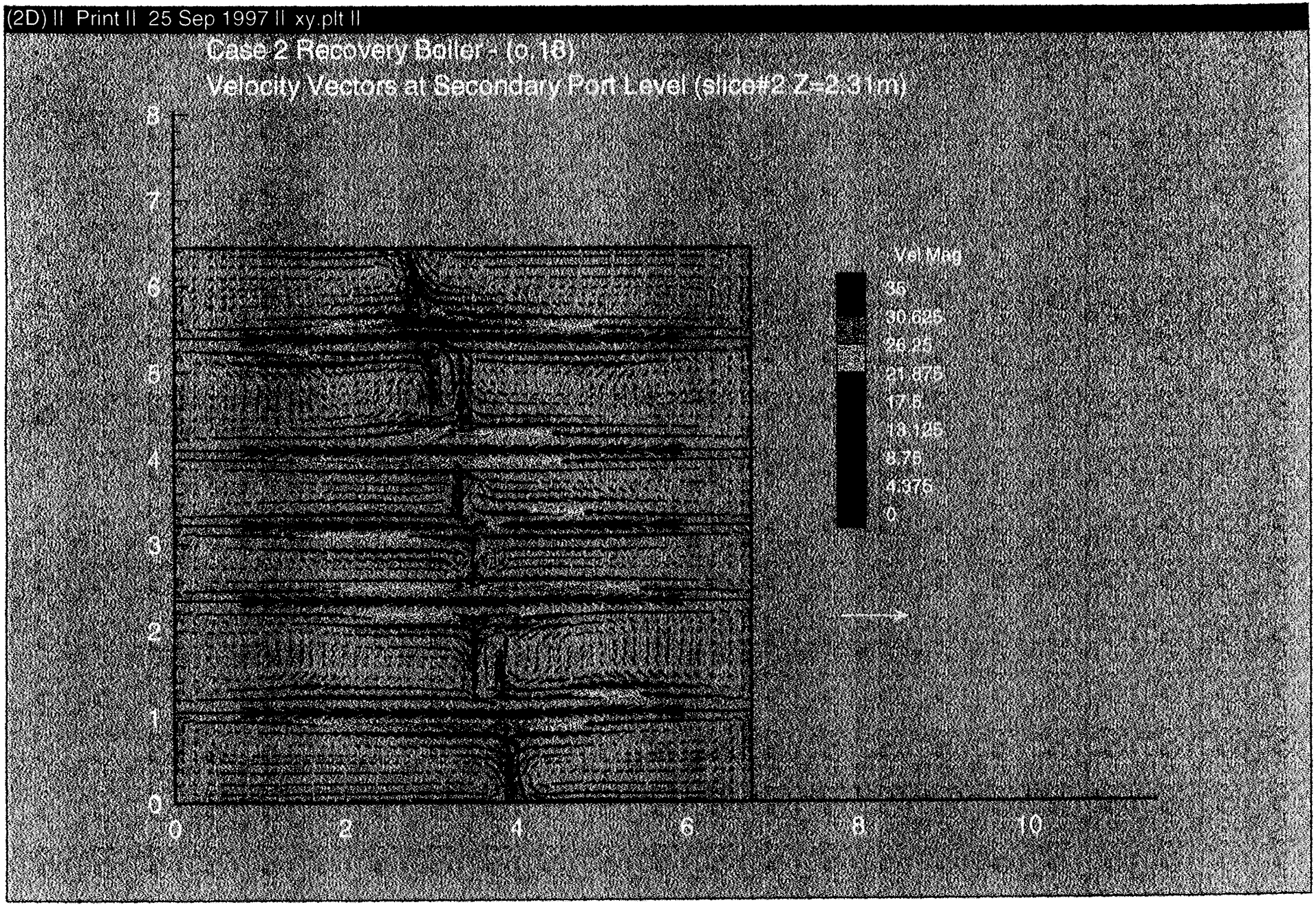

Figure 19. Case 2 - Velocity Vectors in Plan View at Secondary Elevation.

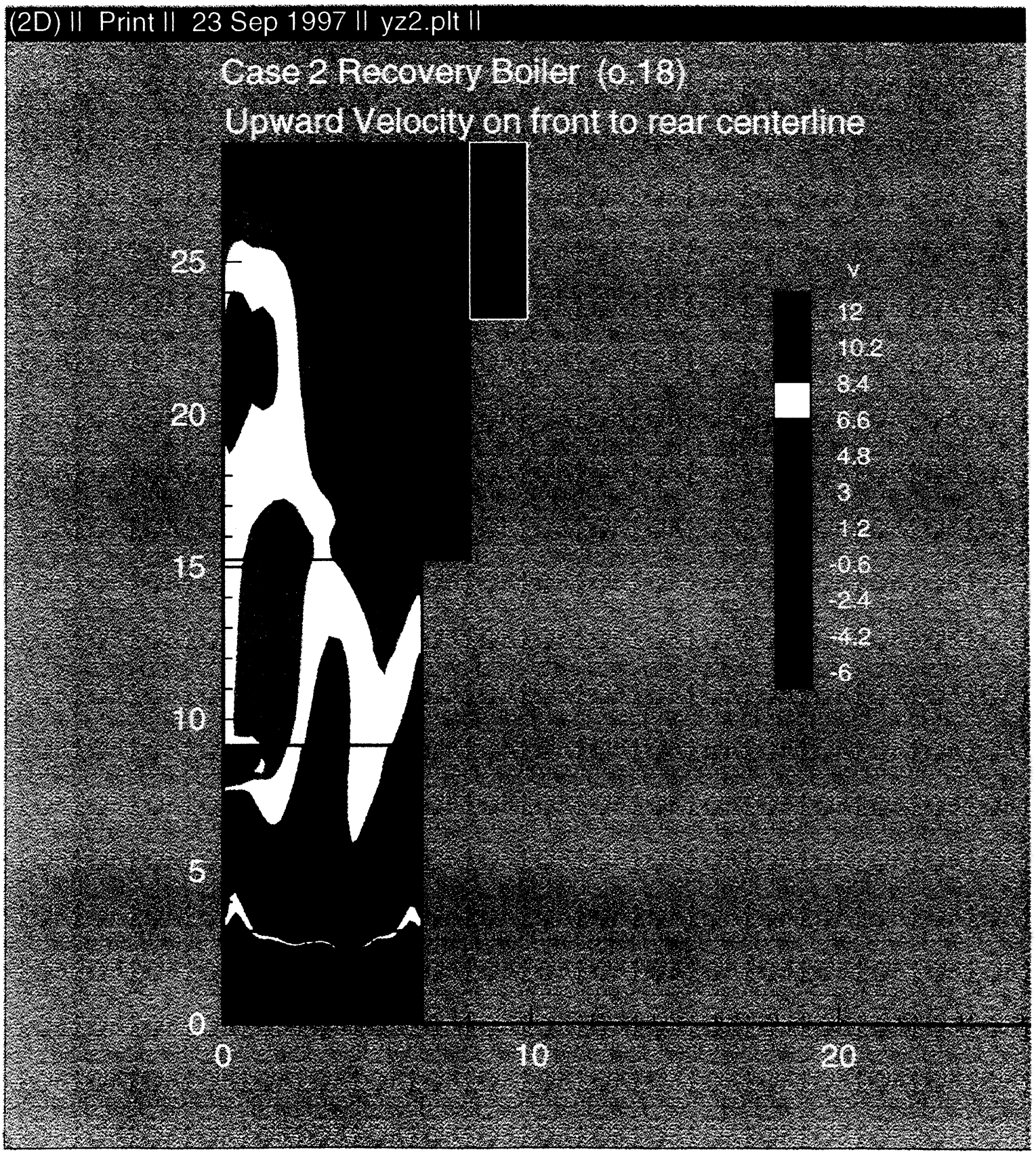

Figure 20. Case 2 - Upward Velocity Contours on Front to Rear Centerline.

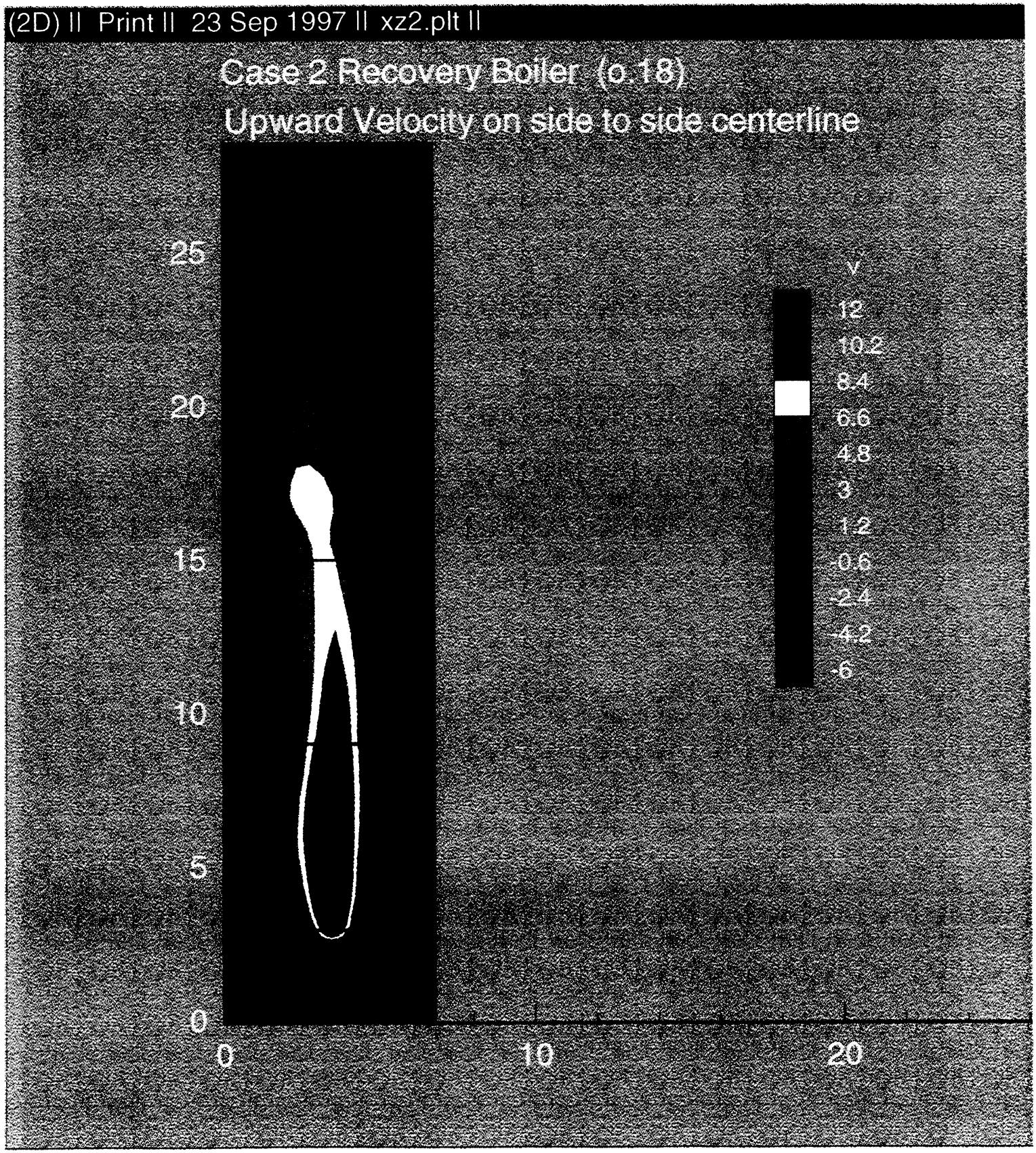

Figure 21. Case 2 - Upward Velocity Contours on Side to Side Centerline.

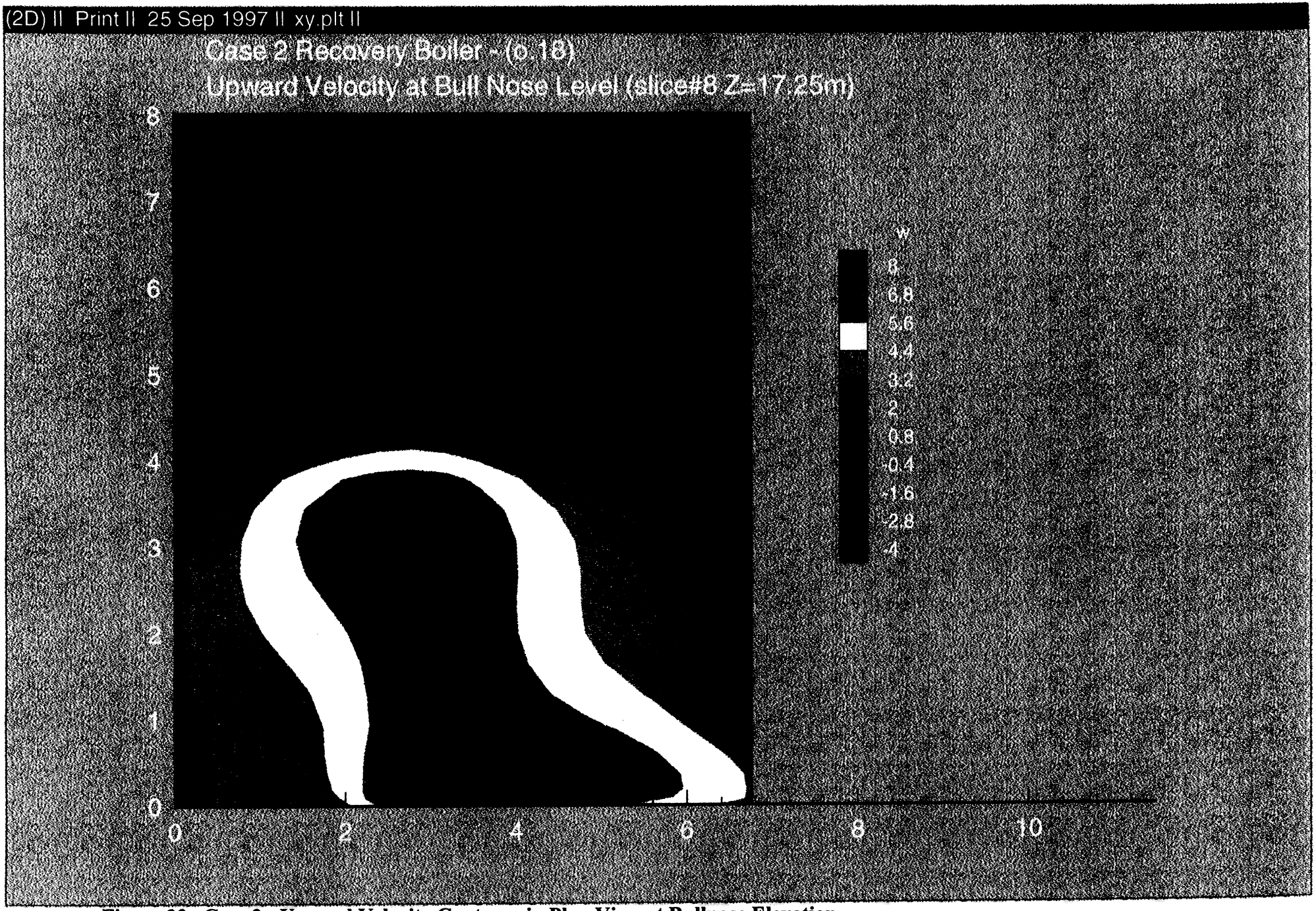

Figure 23. Case 2 - Upward Velocity Contours in Plan View at Bullnose Elevation.

Temperature Profiles

In addition to solving the flow field equations the UBC model also performs energy balances over the entire boiler, so that it is capable of calculating the temperature throughout the boiler. The model includes the energy release and absorption by black liquor during the combustion process, and it accounts for the heat transfer by both convection and radiation. These predicted temperature contours are plotted along the center-line of the boiler in a side view (Figure 24) and a front view (Figure 25). Both the orientation and the location of these slices are the same as used for the velocity profiles in Figures 20 and 21.

The shape of the temperature profiles are strongly influenced by the flow patterns in the furnace. In the lower furnace the highest temperatures are seen near the central high velocity core. The high velocity secondary jets create a zone of turbulence just above the char bed where the highest heat release rates occur. As a result, this gas is heated and continues to flow upward in a central core as described above. As the gas travels farther up in the furnace, the temperature drops and the profile becomes more uniform due to heat transfer to the water walls of the boiler.

Temperatures range from as high as 1700 C in the lower furnace near the char bed, to 550 C near the generating bank in the upper furnace. Overall the temperatures appear to be reasonable, but slightly higher than expected. The average temperature at the bullnose plane is about 1025 C. As was seen in Case 1, the temperature leaving the furnace cavity appears to be too high and the amount of cooling which occurs in the upper furnace is greater than expected. As a result, the temperature entering the generating bank is lower than expected.

The temperature profile at the bullnose elevations is plotted in Figure 26. This plan view slice is at an elevation of 17.3 m which corresponds to the level of the maximum depth of the bullnose arch. The highest temperatures (> 1075 C) occur in an area near the center and shifted slightly toward the left side of the boiler. This high temperature area corresponds of the region with the highest upward velocities.

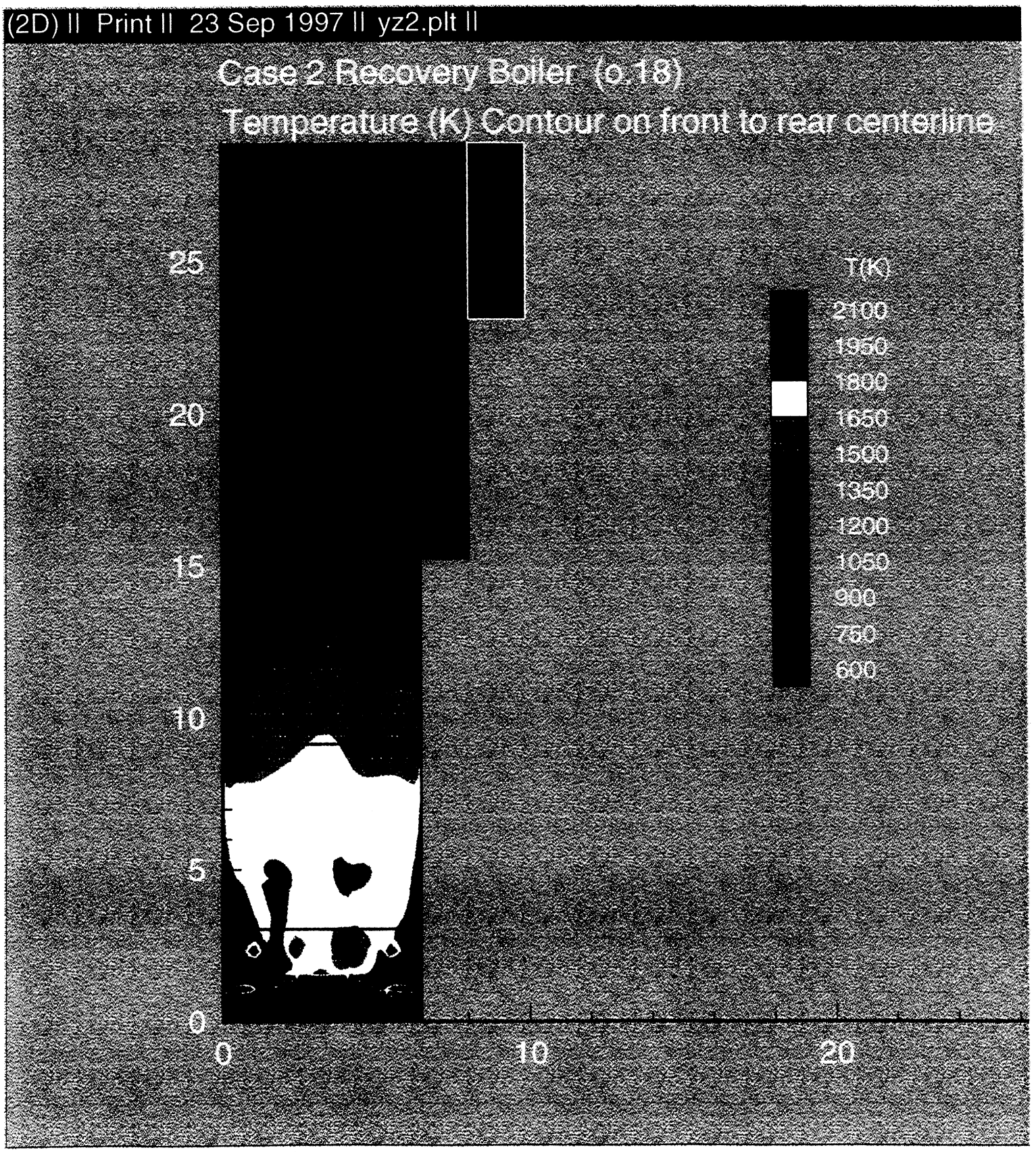

Figure 24. Case 2 - Temperature Contours on Front to Rear Centerline.

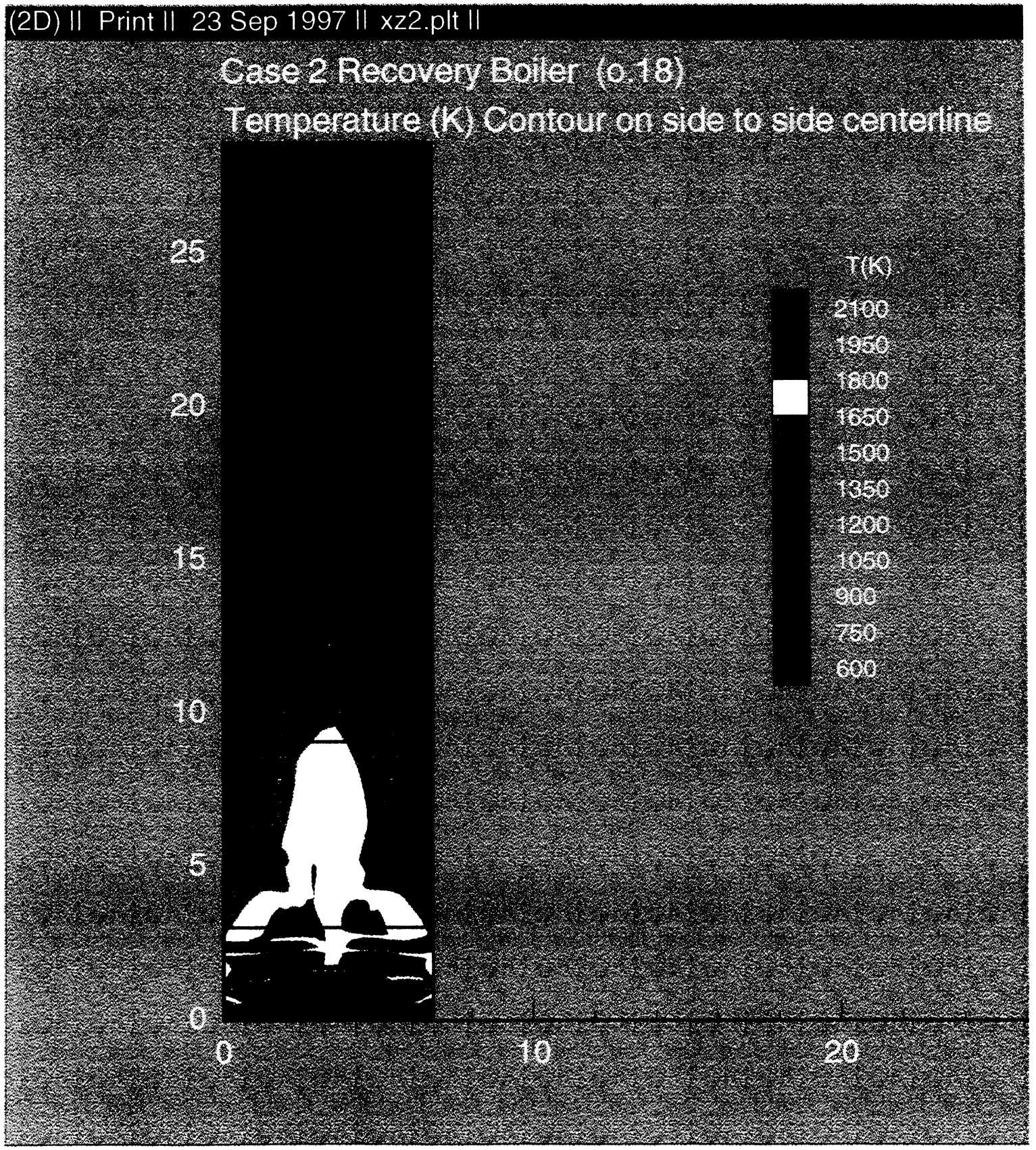

Figure 25. Case 2 - Temperature Contours on Side to Side Centerline.

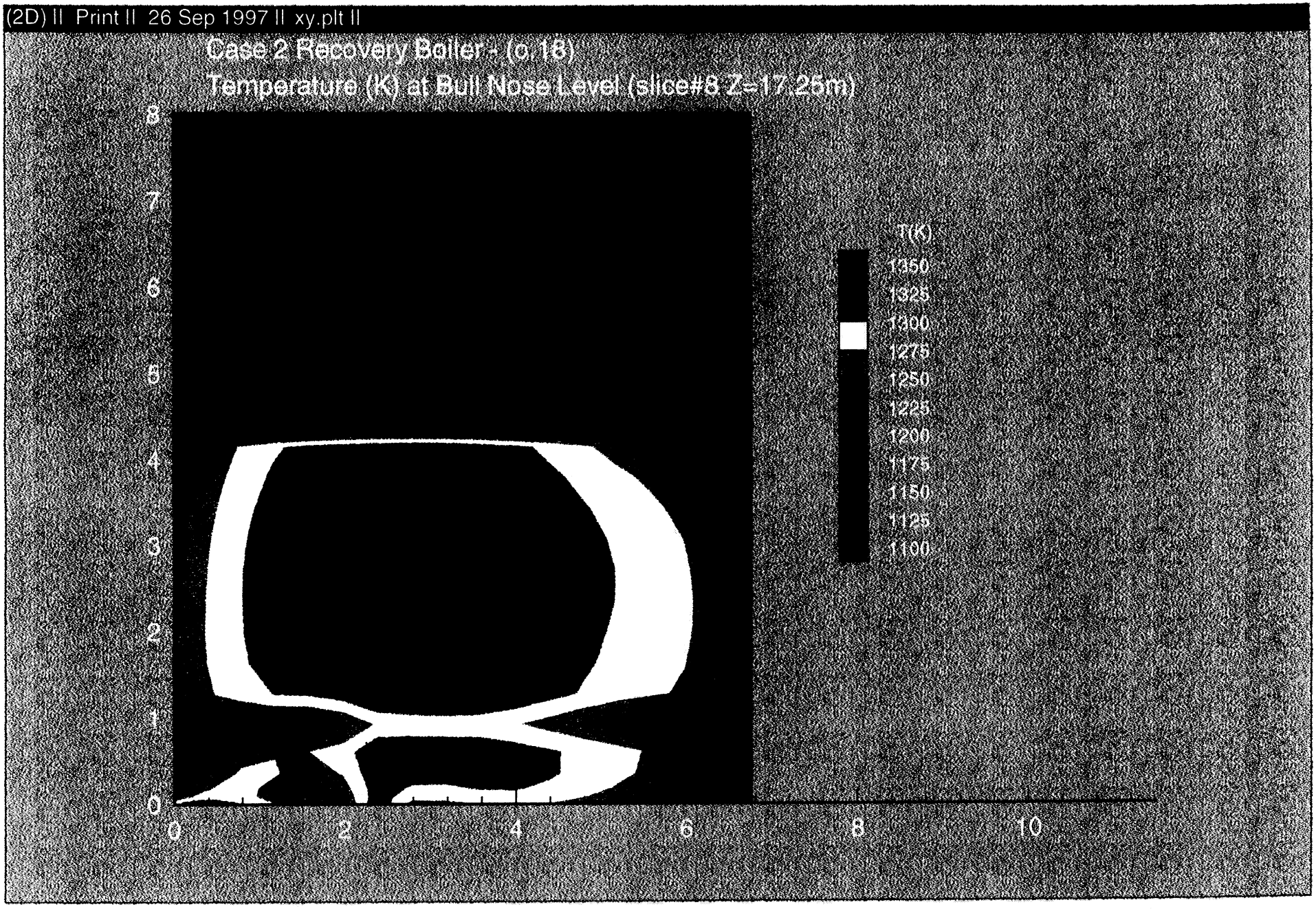

Figure 26. Case 2 - Temperature Contours in Plan View at Bullnose Elevation.

Comparison to Validation Data

During the mill testing performed on this recovery boiler, an attempt was made to collect a large set of data, which would be useful in the testing and validation of computational fluid dynamics based models. Unfortunately, primarily due to the limitations of the recovery boiler model, most of the collected data could not be compared directly with predicted results. For example, the char bed temperatures were measured but are not directly calculated by the model. Also most of the species in the flue gas are not predicted by the model. In addition the gas composition depends on the amount of air leaking into the boiler, which is not accurately known.

As described above, for one of the operating conditions tested at the mill, a corresponding model simulation was set up and solved. For these operating conditions, one set of gas temperature measurements were obtained which provided a direct comparison with the results predicted by this model simulation. Gas temperatures were measured in the upper part of the recovery boiler furnace. In the section below, these results are compared to the values estimated by the recovery boiler simulation.

Gas Temperatures

In the upper furnace above the bull-nose, gas temperatures were measured using an aspirated thermocouple probe under varying operating conditions. Measurements were made on July 17 during test 2a and 2b and on July 18 during test 3a and 3b. Access to the boiler was via three ports located on the front wall of the boiler on the fifth floor, at an elevation of 75ft (22.9 m) above the floor of the boiler. This location is about 17 ft (5.18 m)above the bullnose at the level of the main part of the convective heat transfer sections, directly in front of the screen tubes.

The center port is located on the centerline of the boiler and the other two ports are spaced 5 ft away. The left, center, and right ports correspond to X-direction locations of 6, 11, and 16 ft (1.83, 3.35, and 4.88 m) measured from the left wall of the boiler. The probe was inserted into the boiler in the Y-direction, measured from the front wall. The probe was inserted straight into the furnace (perpendicular to wall) except for a few cases where a small angle was used to vary the X location. The entire probe has a length of about 11 ft (3.35 m) and the probe was inserted from 2 to 8 ft (0.61 to 2.44 m) into the boiler. These readings correspond to locations near the screen tubes and the first set of superheaters. The gas temperature ranged from 680 C to 867 C.

The measurements were performed using a commercial high velocity thermocouple (HVT) probe. In this type of probe the gas is drawn across the tip of the thermocouple to increase the convective heat transfer. As the velocity increases the measured temperature approaches the actual gas temperature. A radiation shield around the thermocouple is also used to reduce the error due to radiative heat transfer. The gas is drawn by a vacuum generated using an ejector driven with compressed air. The probe is constructed of stainless steel and the main section is water cooled.

The measurements, performed at four different boiler operating conditions, are summarized below in Table 8. There does not appear to be any significant variation in the gas temperature due to the change in test conditions. Similarly the variation in the X-direction does not have a statistically significant effect on the temperature. The only variable which appeared to influence the temperature was the Y position (or the extent the probe was inserted in the boiler.) As shown in Figure 27, the temperature seems to have a minimum in the range from 4 to 5 ft (1.22 to 1.52 m) into the boiler. This corresponds approximately to the location of the screen tubes, from 3.5 to 5.5 ft (1.07 to 1.68 m). The screen tubes would be expected to lower the gas temperature near the tubes, due to the increased heat loss as the gas travels upward along the tubes.

Table 8. Upper Furnace Gas Temperatures

Test Run	Port Location	Y Depth (ft)	X Position (ft)	Gas Temp (C)	Test Run	Port Location	Y Depth (ft)	X Position (ft)	Gas Temp (C)
Run 2a	7/17/96				Run 3a	7/18/96			
2a	Front-Left	2.5	6	760	3a	Front-Center	2.8	10	808
2a	Front-Center	2.5	11	730	3a	Front-Left	3.0	5.5	781
2a	Front-Center	2.5	11	740	3a	Front-Center	3.0	11	751
2a	Front-Right	2.5	16	840	3a	Front-Right	3.0	16	741
2a	Front-Center	4.5	11	750	3a	Front-Center	4.8	9.5	731
2a	Front-Center	6.5	11	840	3a	Front-Left	5.0	6	686
					3a	Front-Right	5.5	16	741
Run 2b	7/17/96				3a	Front-Left	6.5	6	795
2b	Front-Left	2.5	6	750	3a	Front-Center	6.7	9	813
2b	Front-Center	2.5	11	800	3a	Front-Right	7.5	16	798
2b	Front-Center	2.5	11	740	3a	South wall	16.0	15.5	628.5
2b	Front-Right	2.5	16	725	3a	South wall	16.0	18	598
2b	Front-Right	4.0	16	750					
2b	Front-Left	4.5	6	680	Run 3b	7/18/96			
2b	Front-Center	5.0	11	810	3b	Front-Left	2.50	6	775
2b	Front-Left	6.0	6	810	3b	Front-Center	3.35	12	705
2b	Front-Right	6.5	16	773	3b	Front-Right	3.50	16	811
2b	Front-Center	7.0	11	820	3b	Front-Left	5.00	6	799
2b	Front-Center	7.0	11	773	3b	Front-Center	5.29	12.5	700
2b	Front-Right	8.0	16	780	3b	Front-Right	6.00	16	748
					3b	Front-Left	7.00	6	867
					3b	Front-Center	7.23	13	790
					3b	Front-Right	7.50	16	804
					3b	South wall	16.0	15.5	548
					3b	South wall	16.0	18	541

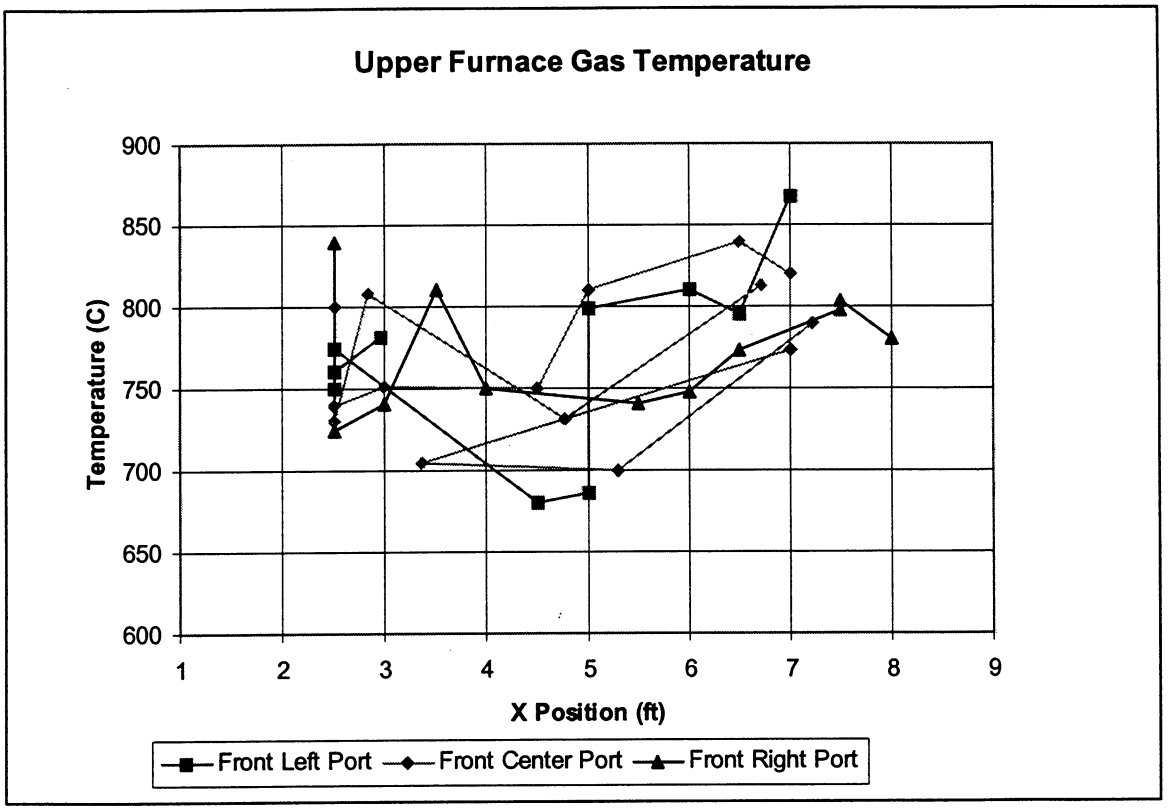

Figure 27. Upper Furnace Gas Temperatures.

As described in the previous section, the model also predicts the gas temperature at these same locations. The temperature contours are graphed below in Figure 28 for the elevation of the access ports (z=22.86 m). It can be seen that at this elevation the highest temperatures exist near the front wall of the boiler. The peak temperatures are located at a position to the left of center at x=2.0 m. This offset in the location of the peak temperature corresponds to the offset in the peak velocity toward the left side of the boiler. This figure shows a drop in temperature which corresponds to the location of the screen tubes. The overall temperature in the region where measurements were made is about 867 C (1140 K).

Finally the predicted gas temperatures are plotted alongside the measured gas temperatures for the same location in the boiler, providing a direct comparison. Three separate plots are shown which correspond to the data from the left side port (Figure 29), the center port (Figure 30) and the right side port (Figure 31). The average measured temperature of 771 C is about 92 C lower than the predicted average temperature of 863 C. One the left side of the boiler the difference is the largest, the average measured temperature of 770 C is 138 C lower than the computed value of 908 C. In the center port the average value of 767 is 108 C less than the calculated value of 875 C. On the right side the difference is only 34 C, with an average measured value of 775 C and an average calculated value of 809 C.

It is not clear what causes this fairly large difference between the measured and computed temperatures. It may that there is a problem in the overall energy balance which over-predicts the recovery boiler temperatures. Or it may be due to the definition of boundary conditions for the temperature of the walls or the heat exchange sections of the boiler. The model also predicts higher temperatures on the left side of the boiler, which are not seen in the measured temperatures. This high temperature region may be caused by the drift of the high velocity core which was described in the simulation results of the previous section.

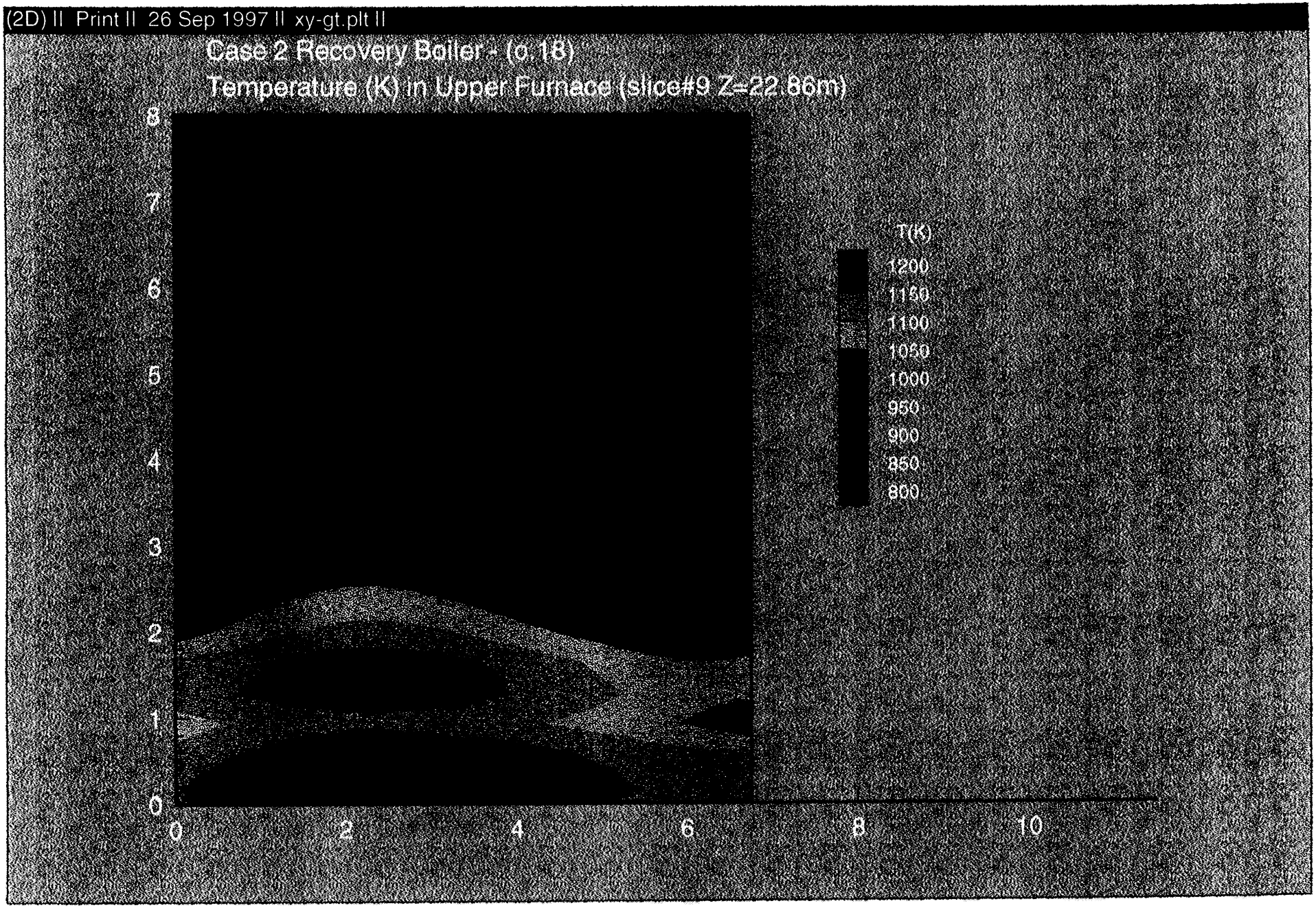

Figure 28. Case 2 - Temperature Contours in Upper Furnace in Plan View at Z = 22.9m.

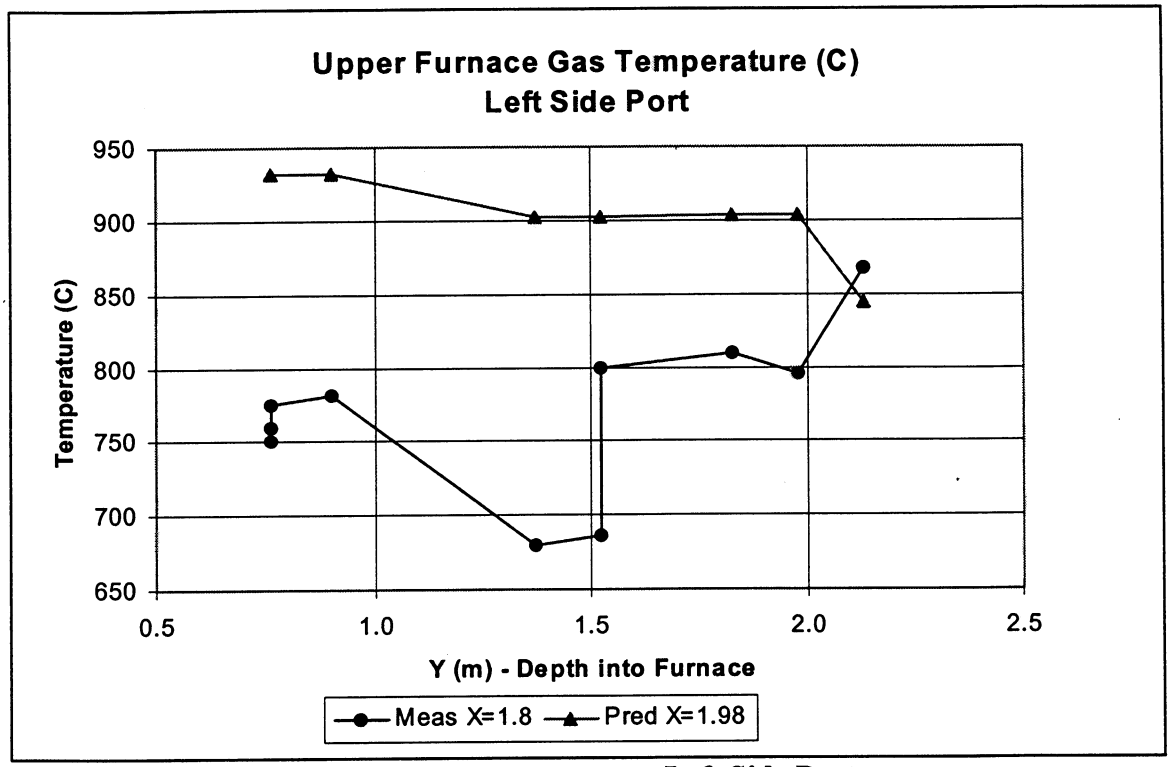

Figure 29. Upper Furnace Gas Temperatures - Left Side Port.

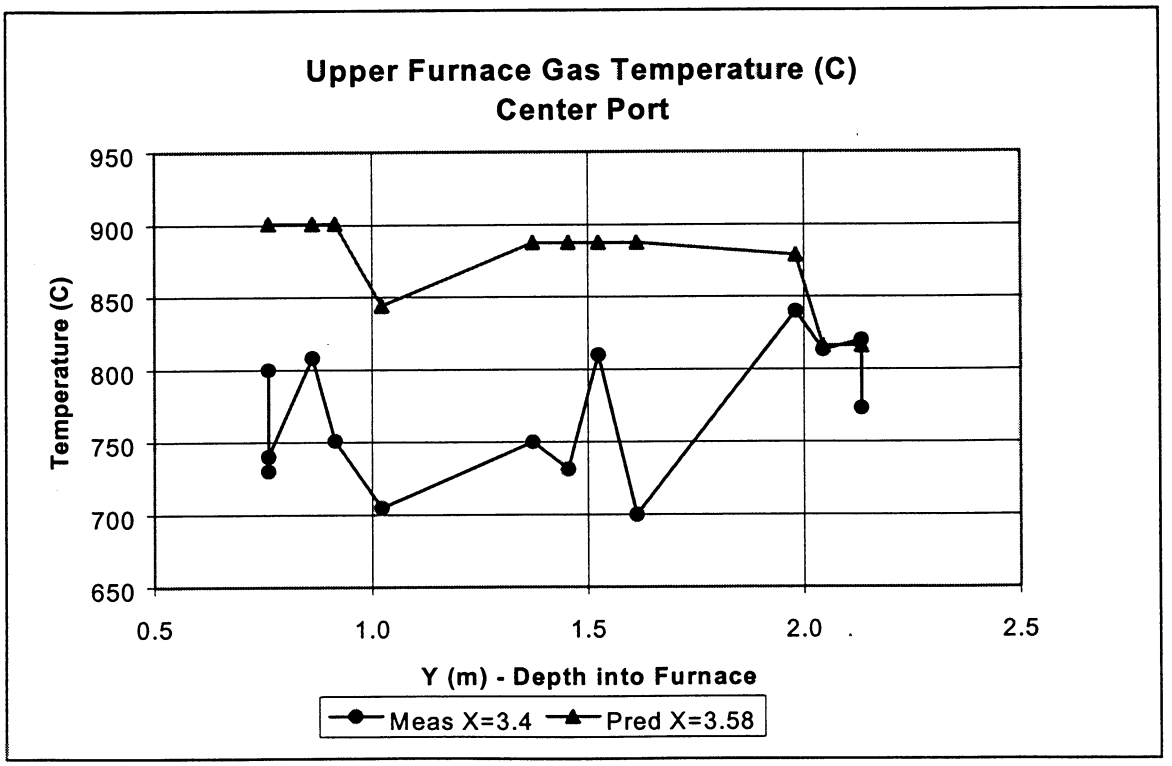

Figure 30. Upper Furnace Gas Temperatures - Center Port.

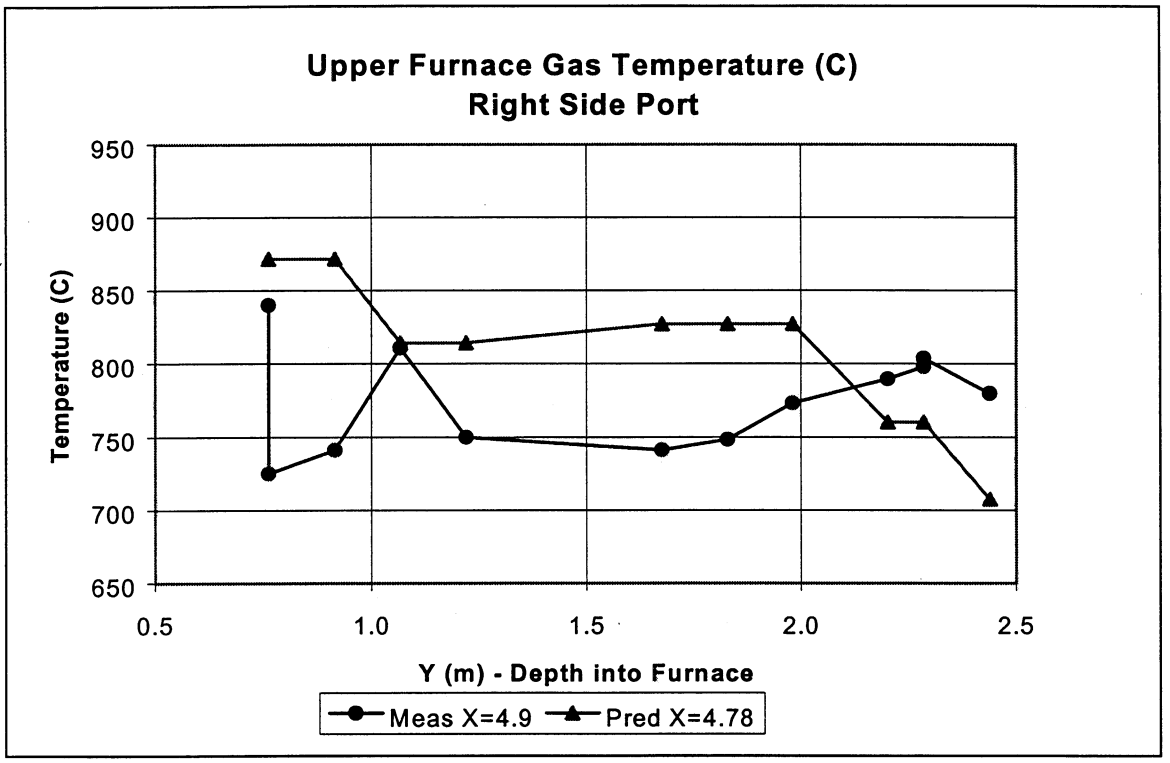

Figure 31. Upper Furnace Gas Temperatures - Right Side Port.

Four additional readings were taken at a port on the right (south) wall of the boiler on the fifth floor. This port is located about 16 ft from the front wall of the boiler at an elevation of 72 ft above the floor of the furnace. As expected the temperature is lower at this point which is closer to the generating bank. The average measured temperature of 579 C is very close to the average predicted temperature of 570 C.

One other piece of information was collected at the recovery boiler which can be used to validate the recovery boiler simulation. From visual observation through the front wall access ports, the gas flow appeared to go straight up with few indications of cross flow. Very few sparklers or signs of carryover could be seen. None were seen in the right port and only a few were noted in the left port. The flow also appeared slightly more turbulent in the left port. This observation agrees with the general flow patterns predicted by the model. The high velocity core tends to move toward the left side of the boiler in the upper furnace. This higher velocity would be expected to produce higher levels of carryover.

Case 3 - Benchmarking Exercise - Water Model Studies

A third case was used for validation of the flow field predictions from the UBC CFD model. In this case an isothermal flow experiment was carried out at UBC on a scale model of a Babcock & Wilcox recovery boiler. Measured velocity profiles from the 1:28 scale model recovery boiler were compared to the computational model predictions. The results of this study are included as a separate appendix in this DOE report (Modeling of Black Liquor Recovery Boilers by Salcudean et al.).

As a benchmarking exercise, a second CFD simulation was also performed using the commercial CFD software package, Fluent. This simulation was based on the same physical water model described above. These Fluent results are compared to both the measured velocities from the physical model and the predicted velocities from the UBC model.

Model Setup and Solution

The two models applied are based on the use of computational fluid dynamics (CFD) and both require a similar procedure for defining and solving the models. The first step in the setup is to define a three-dimensional grid which reflects the geometry of the boiler. The second step is to define the conditions at the limits of the boiler, i.e., the boundary conditions and the initial conditions for the model. The final step is the actual solution of the mass, momentum and heat transfer balances, which is performed in an iterative method.

Geometry and Grid

Physical Model

The model boiler is a water model on a 1:28 scale of a recovery boiler located at a Weyerhaeuser mill in Kamloops, British Columbia. The model walls are constructed of 16 mm thick plexiglass, so that laser light can be transmitted freely through to the measurement locations, to allow laser doppler velocimeter measurements at different elevations. Water is used as the flow fluid in the model and is injected at three elevations, which correspond to the three air levels in the actual boiler. The furnace model includes a sloped floor at the base, and the bullnose and heat exchangers in the upper section of the furnace. A schematic diagram of the model is given in Figure 32.

Figure 33 displays a profile of the recovery boiler model showing the elevations of the injection ports, the dimensions of the bullnose, and the locations of the three levels (#1, #2, #3) where laser doppler velocimetry (LDV) measurements were taken. The model boiler has a sloping floor and the primary injection ports are inclined from the front to the back of the model.

The 174 primary air ports are nearly evenly distributed around the perimeter of the furnace. At the secondary air elevation, four ports are located on the front and back walls, and five on the left and right. Also included at this elevation are two large starting burners on each of the front, left and right walls. The tertiary air is distributed in an interlaced fashion, with four ports on the front wall and five on the back.

Detailed drawings of the boiler are presented in the paper referenced above (Salcudean), which are suitable for use in a CFD modeling exercise. Included in this report are figures showing the positions and dimensions of the primary, secondary, and tertiary injection ports, respectively.

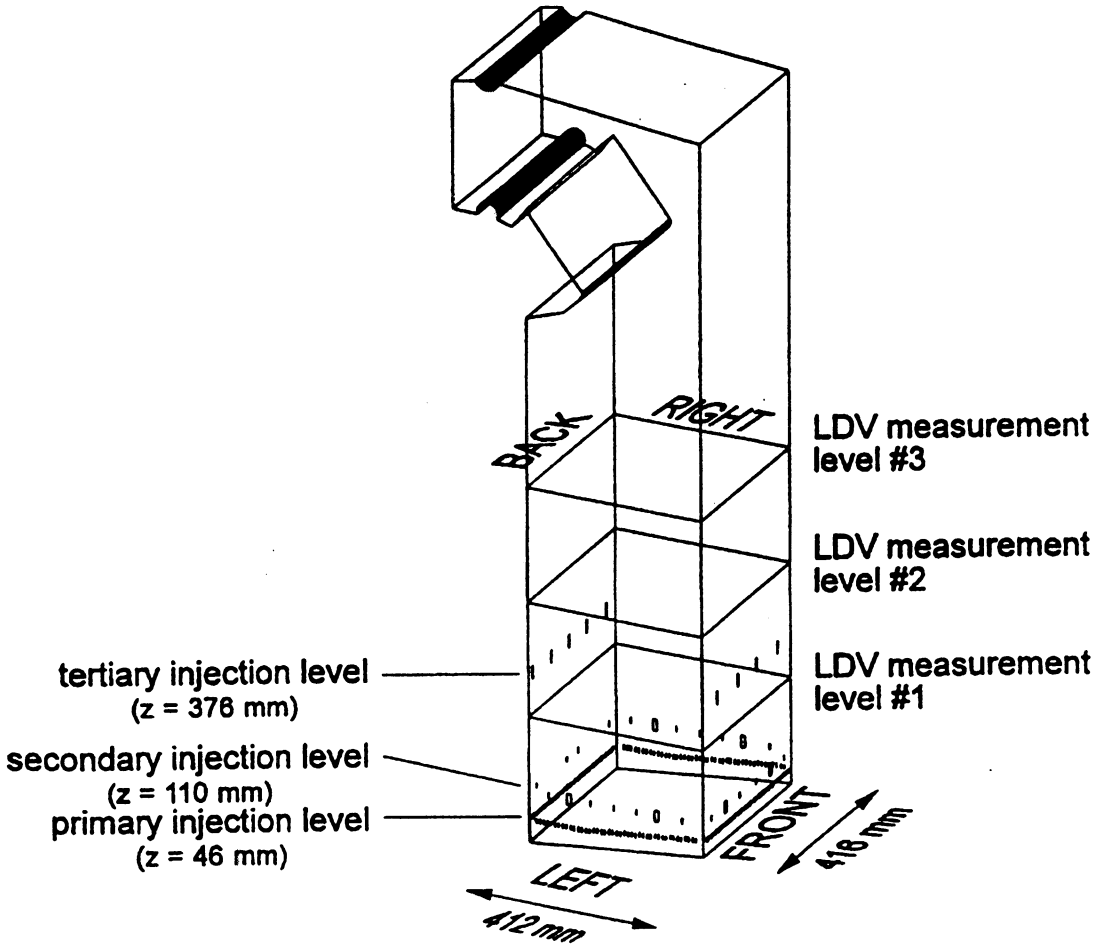

Figure 32. Schematic Drawing of the Case 3 Recovery Boiler Water Model.

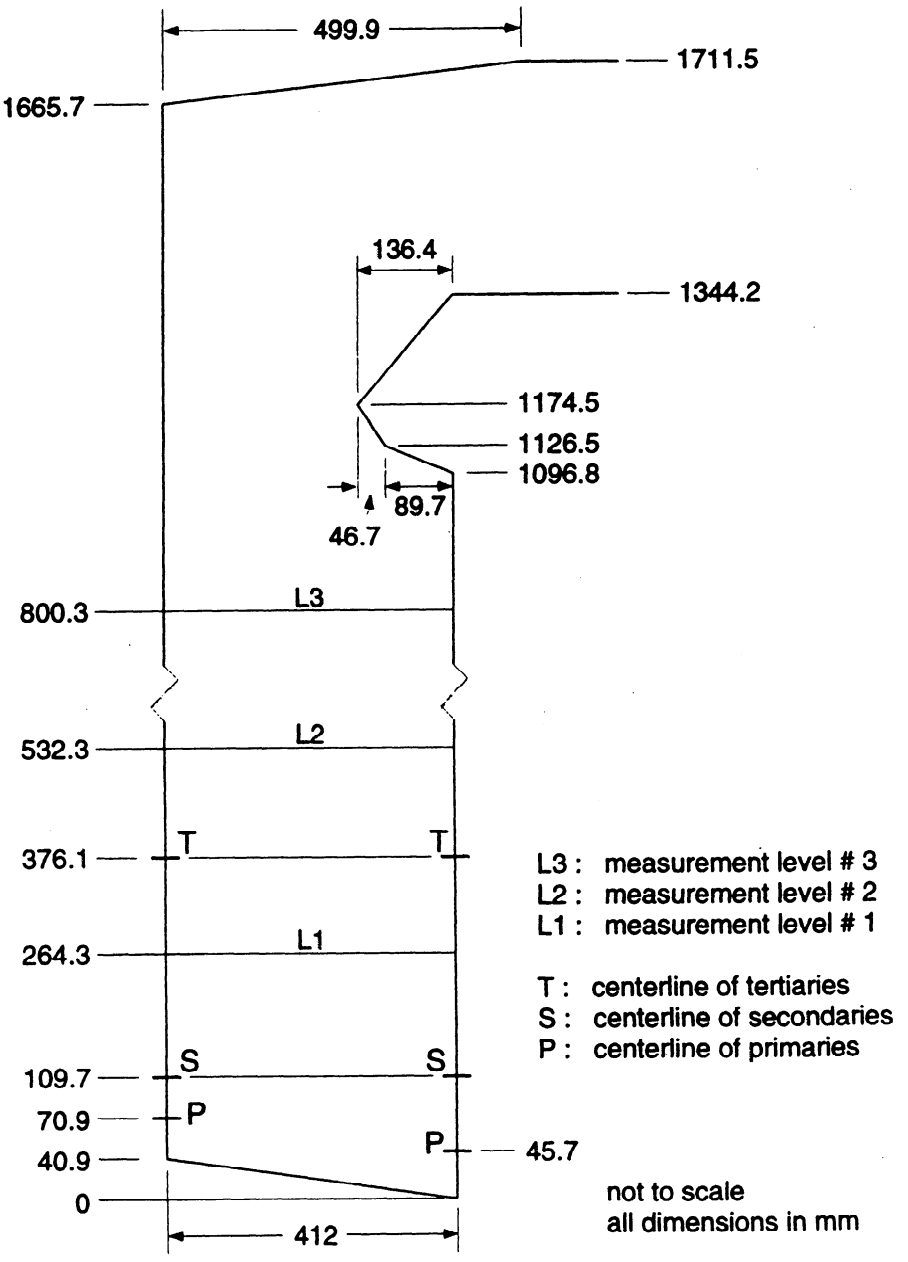

Figure 33. Case 3 Recovery Boiler Water Model: Vertical Cross-Section.

UBC Model

The setup of the grid for the UBC simulation includes the upper furnace region with the bullnose and the heat exchangers. The outlet for the simulation is at the outlet of the generating bank of the furnace. The sloped floor is also included in the model. Detailed information on the setup of this model is contained in the report by Salcudean.

To simplify the setup of the grid, the primary ports are represented as long slots, rather than each of the individual ports. The primary ports on the front and rear walls are modeled as a single slot, since all the openings are at the same elevation. The primary ports on the side walls along the slope of the furnace floor are modeled as 4 separate slots to account for the change in elevation along the sides. The same total open area for the primary ports has been maintained in the setup. The secondary port and the starter burner openings are modeled as rectangular openings, and they match the size and shape of the physical model.

Fluent Model

The Fluent model of this recovery boiler was setup using a cartesian coordinate system. The grid is 54 x 42 x 57 for a total of 129,297 cells. The overall arrangement is shown in Figure 34. The sloped floor was created by using a stair-step arrangement. This model did not include the heat transfer region in the upper furnace. The model was limited to the region below the bullnose and the outlet corresponds to the gap between the front wall of the furnace and the bullnose arch.

Due to the large number of primary ports, the individual ports were combined so that groups of seven or eight ports are represented as a single slot. These groups of primary ports correspond to the ports that are fed by a single water line and control valve. Therefore the initial velocities are equal for all the ports within these groups of ports. Although the shape of the primary ports has been modified, the port area has been maintained so that the initial velocity and the inlet mass flux match those in the physical model. The overall location and arrangement of these ports closely matches that of the physical model. Previous work has shown that the use of a long slot in place of the individual primary air ports has very little impact on the overall flow field.

The arrangement of the primary and secondary ports is shown more clearly in the side view of the lower half of the boiler in Figure 35. The standard secondary ports in the model are very close in size, shape and position to those in the physical model. The large starter burner ports are modeled accurately in terms of area, but the orientation has been changed so that they are wider and shorter. This was necessary due to the limitations on the overall number of cells. With the relatively low inlet velocity from the starter burner ports the change in shape should not have a large impact on the overall solution.

The physical model includes five tertiary ports on the rear wall and four on the front wall. For the case where measurements were made no flow was used at this level. Therefore the tertiary ports were not included in the Fluent model.

Inlet Conditions

Physical Model

The experiment considered was as follows: the total volume flow rate through the model was set to 570 L/min, and the flow was through primary and secondary ports only. Approximately 61% of the flow was diverted to the primary ports and the remaining 39% went to the secondary ports; there was no tertiary injection.

The flow system for the model was designed such that at the secondary elevation, water is supplied to each port by its own line. At the primary elevation, however, flow to the 174 ports was supplied by only 24 lines, each of which fed a group of 7 or 8 ports. Figure 36 shows the volume flow rates and momentum fluxes at the primary and secondary levels.

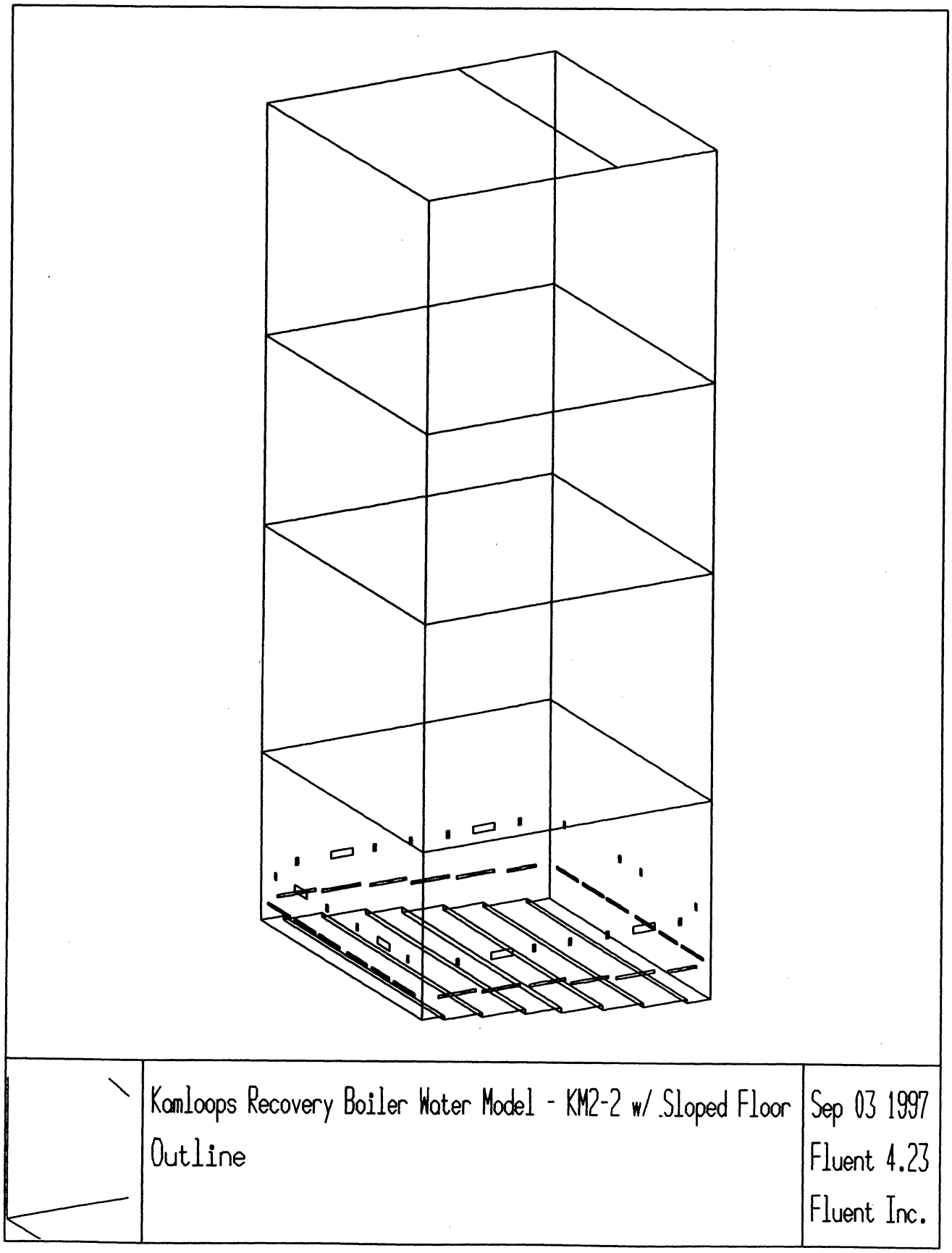

Figure 34. Fluent Model of the Case 3 Recovery Boiler Water Model.

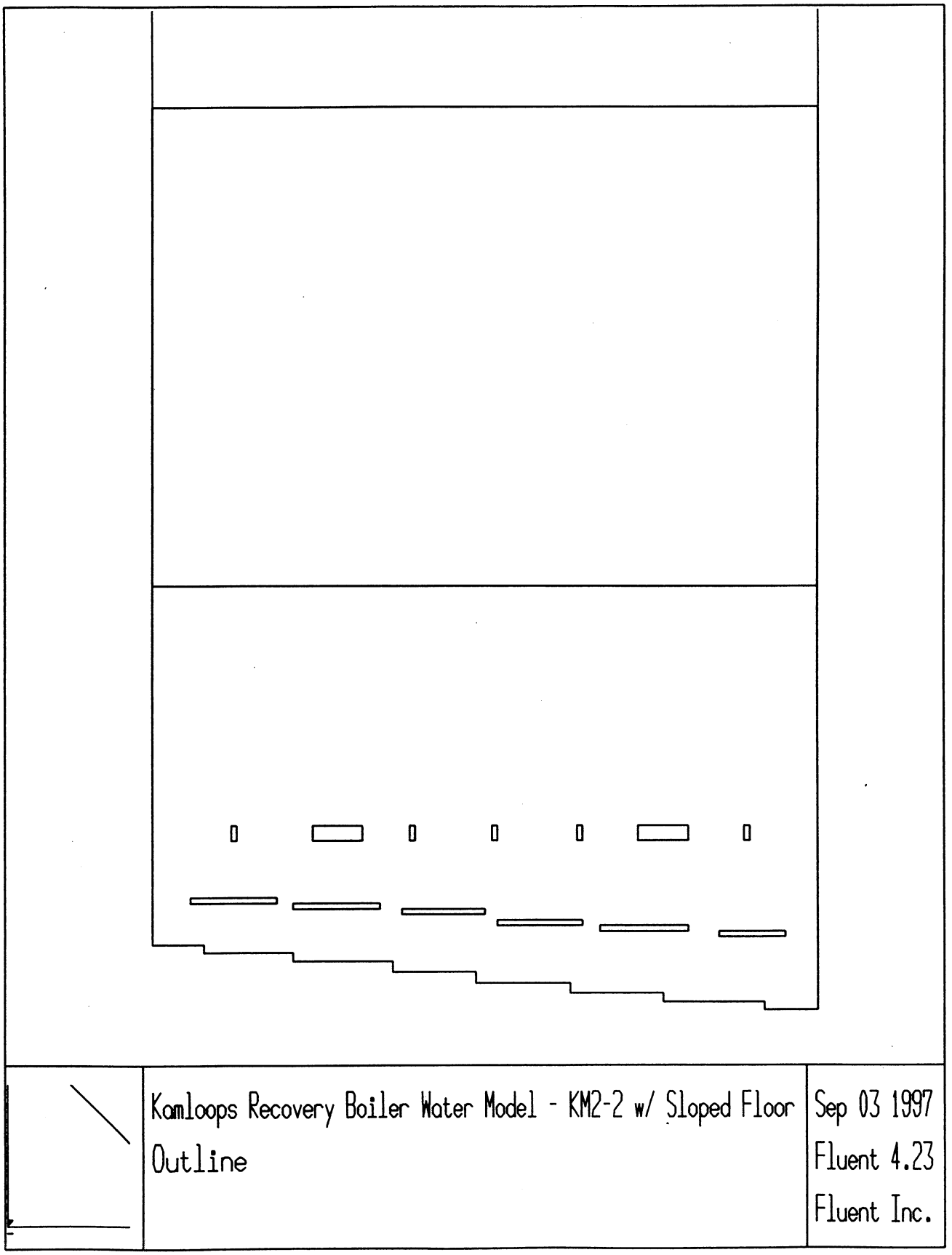

Figure 35. Fluent Model of the Case 3 Recovery Boiler - Side View.

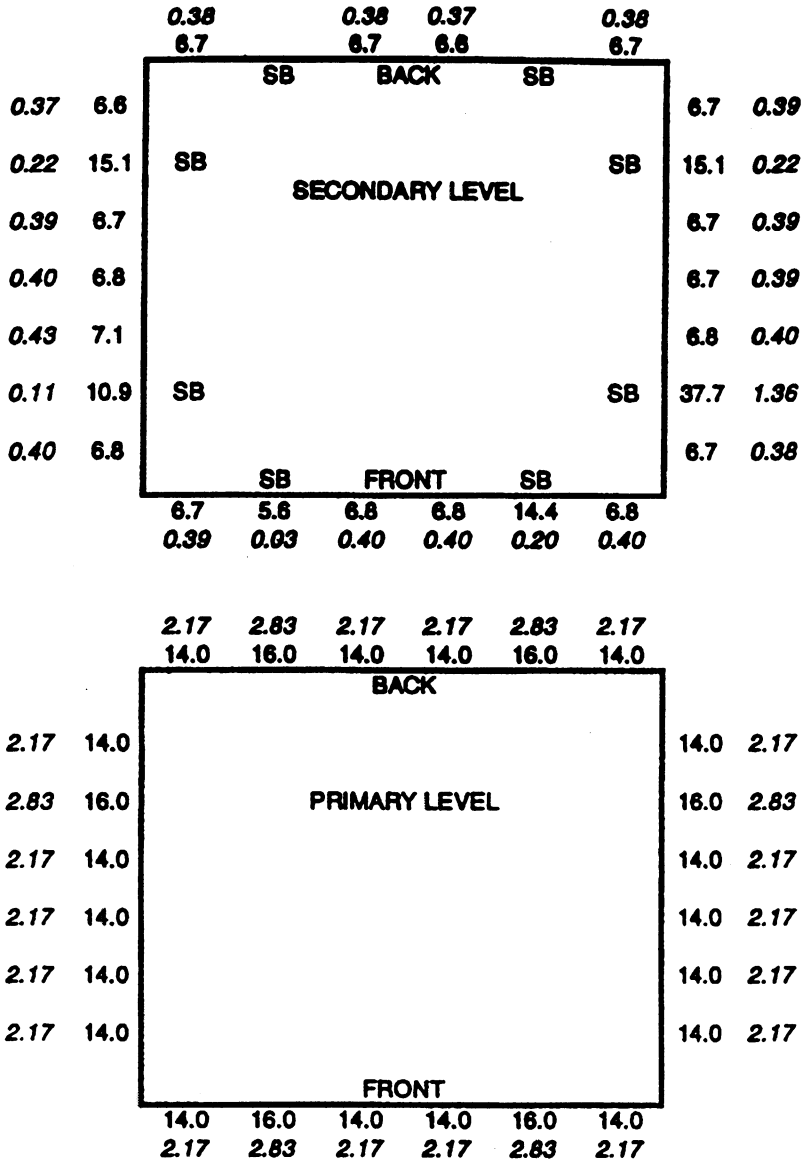

Figure 36. Flow-rates for the Case 3 Recovery Boiler Water Model.

UBC Model

The inlet jet velocities were calculated based on the experimental mass flow rates. From the measured flow rates and dimensions of each individual port, a velocity value can be calculated for the flow through each port. A summary of these values is shown below in Table 9. At the primary level, the flow-rates to the ports are uniform for the entire boiler so the inlet velocity is a constant value of 1.33 m/s. For the secondary jets a typical velocity was 3.65 m/s. For the starter burners a typical velocity was 0.624 m/s.

Turbulence intensity for primary jets was 10%; that is, $k = 0.1 * V * V$. Turbulence intensity for secondary jets and starter burner jets was 1.0%; that is $k = 0.01 * V * V$. A higher value was used for the primary jets because the jets were modeled as slot jets, and so the turbulence intensity was increased artificially to compensate for the differences and physical characteristics. Constant properties of water were used in the simulation. The density was 998.2 kg/m^3 and the dynamic viscosity was 0.00098 kg/m/s.

Table 9. Inlet Port Velocities

		No. of Ports	Area (cm^2)	Flow (L/min)	Velocity (m/sec)
Primary Ports					
Left		43	10.780	86	1.330
Right		43	10.780	86	1.330
Front		44	11.031	88	1.330
Rear		44	11.031	88	1.330
Total		174	43.622	348	1.330
				61.2%	
Secondary Ports					
Left	Regular	5	1.625	34	3.487
	Starter	2	5.805	26	0.746
	Total	7	7.430	60	2.117
Right	Regular	5	1.625	33.6	3.446
	Starter	2	5.805	52.8	1.516
	Total	7	7.430	86.4	2.481
Front	Regular	4	1.300	27.1	3.474
	Starter	2	5.805	20	0.574
	Total	6	7.105	47.1	2.024
Rear	Total	4	1.300	26.7	3.423
Total		24	23.266	220.2	2.511
				38.8%	

Fluent Model

At the secondary level there is significant variation in the velocity from port to port. The standard secondary ports have an average velocity of 3.5 m/s. The starter burners are larger so that the velocity leaving these ports is lower, 0.95 m/s on average. In the Fluent model the inlet velocities for the secondary ports are set at a constant value for each side of the boiler and the starter burners are set individually. A turbulence intensity of 10% was assumed for all inlet flows. A constant density of 1000 kg/m^3 and a constant viscosity of 0.001 kg/m/s were used in the Fluent model.

Simulation Procedure

UBC Model

For the UBC Case 3 model, the simulation was first calculated as a steady-state model for about 1500 iterations. Subsequently it was run as a transient model; with a time step of 1.0 second. Five or six time steps (each 500 iterations) were required to reach a final steady-state solution. The flow field was visually constant for the last few time steps.

Fluent Model

The Fluent model was run for 5000 iterations and it was found that the residuals were continuously decreasing during the first 2500 iterations. After this the residuals remained approximately constant despite changes made in the under-relaxation values. The minimum sum of the normalized residuals was 4.3 x 10-3. Although this is slightly higher than the default convergence criteria (10-3), based on a visual examination of the flow fields, the solution appears to have reached a steady-state, consistent with a converged solution.

Experimental conditions and flow measurements

Measurements were acquired in three evenly spaced horizontal planes. Each plane was divided into a 6x6 grid of rectangular cells with the measurement locations corresponding to the cell centers. The lower plane was located at the liquor gun elevation, at an elevation of 264 mm (measured from the lowest level of the floor) or 155 mm above the secondary ports. The middle plane was located at an elevation of 523 mm, approximately the same distance (156 mm) above the tertiary ports. The upper plane was located at 800 mm elevation, 425 mm above the tertiary ports. These three planes are referred to as levels 1, 2 and 3, respectively (shown earlier in Figure 33).

As a first order verification of the LDV measurements, the total flow through a horizontal section was calculated by summing the individual measured flows through each cell in the 6x6 grid. A volume flow rate was calculated for each of the measurement levels with the results summarized in Table 10.

Table 10. Measured vs. Set bulk volume flow

Location	Set bulk flow across the level [L/min]	Measured bulk flow [L/min]	Percent error in measurement
Level 1	570	754	+32%
Level 2	570	641	+12%
Level 3	570	656	+15%

The general disagreement may be attributed to the following factors:

1. The measurement grid is rather coarse and may not well represent some of the lower velocity regions.
2. Turbulence levels, in particular at level 1, are high, and may lead to significant errors in flow statistics.
3. Operation of the LDV data acquisition equipment with less than extreme care may have led to a systematic filtering of signals corresponding to low velocity measurements.

At higher elevations, the error is not as significant, and probably has little effect on the information retrieved from the data with respect to the observed trends and large scale patterns in the flow field.

Flow Fields Results and Comparisons

In addition to the experimentally determined velocity measurements, flow fields were also computed using two different CFD simulations. The first simulation was performed using the UBC code to predict the flow patterns in the Case 3 recovery boiler water model. A second CFD simulation was performed using the commercial CFD code Fluent to predict the flow fields. In the following section the experimental results are compared to the predictions from the UBC model. Finally, the flow field results from the Fluent model are presented and compared to both the experimental data and the UBC model results.

Experimentally Measured Flow Fields vs. UBC Model Numerical Results

Measurements made for the flow field reveal the following general features: at level 1 there is a strong upward flow core, mostly in the central region, but deflected somewhat towards the rear-left corner. A downward flow region exists in the right front corner. At level 2 the high velocity upward flow has spread outward and is distributed along the left and rear walls. The downward flow region is now located in the right front corner, but shifted slightly along the front wall towards the center. At level 3 the down flow region has spread out slightly, but is still located in the right front corner. The upward flow remains strong along the left wall and but only extends about 2/3 of the way along the rear wall.

Figure 37 shows the distribution of the upward velocity component at level 1, above the secondary elevation, for both the measured and the calculated flow fields. There is general agreement between the two flow fields; both show an upward flow close to the left side wall, and downward flow along the right wall, closer to the front wall. In both, the overall shape and location of the upward velocity region is quite similar. The down-flow region for the numerical results is slightly larger and extends farther into the upper right corner. The small circles on the left image indicate the 6 by 6 measurement grid.

Figure 38 shows the vertical velocity distribution at level 2, above the tertiary ports. Although similar features in the flow field can be seen in both the experimental and numerical results - an upward flow in the rear left half of the model and downward flow in the front right half - there is more difference between these two flow fields than at level 1. The up-flow region of the measured results is closer to the wall than the numerical data. The down-flow area also has a different shape when these results are compared.

At level 3 the experimental and numerical data show better agreement. Figure 39 shows the velocity distribution at level 3, under the bullnose. Similar velocity fields are found for both cases, with upward flow in the rear left side and downward flow in the front right side.

Fluent Results vs. Measured Flow Fields and UBC Model Flow Fields

At level 1 the Fluent flow field (Figure 40) is very similar to the numerical results from the UBC simulation and is also in good agreement with the experimental data. The up-flow region in the Fluent model is almost identical to the computed results from the UBC model. The vertical velocity from the Fluent results are plotted in units of meters per second. The previous results were graphed in terms of dimensionless velocity based on an average upward velocity of 0.055 m/s. Therefore a dimesionless velocity of 4 corresponds to an actual velocity of 0.22 m/s.

As shown in Figure 41, at level 2 the flow field predicted by the Fluent model is closer to the measured flow field than the predictions from the UBC model. The up-flow region is spread out along the left and rear walls of the boiler. The down-flow region is roughly intermediate to the measured flow field and UBC simulation results.

At level 3 (Figure 42) the Fluent simulation continues to do a good job of predicting the up-flow region, but it appears to be slightly less accurate than the UBC model in predicting the down-flow region. Overall, all three cases show some differences, but are in general agreement in terms of the main flow features, demonstrating the ability of CFD models to predict the general flow behavior in a recovery boiler.

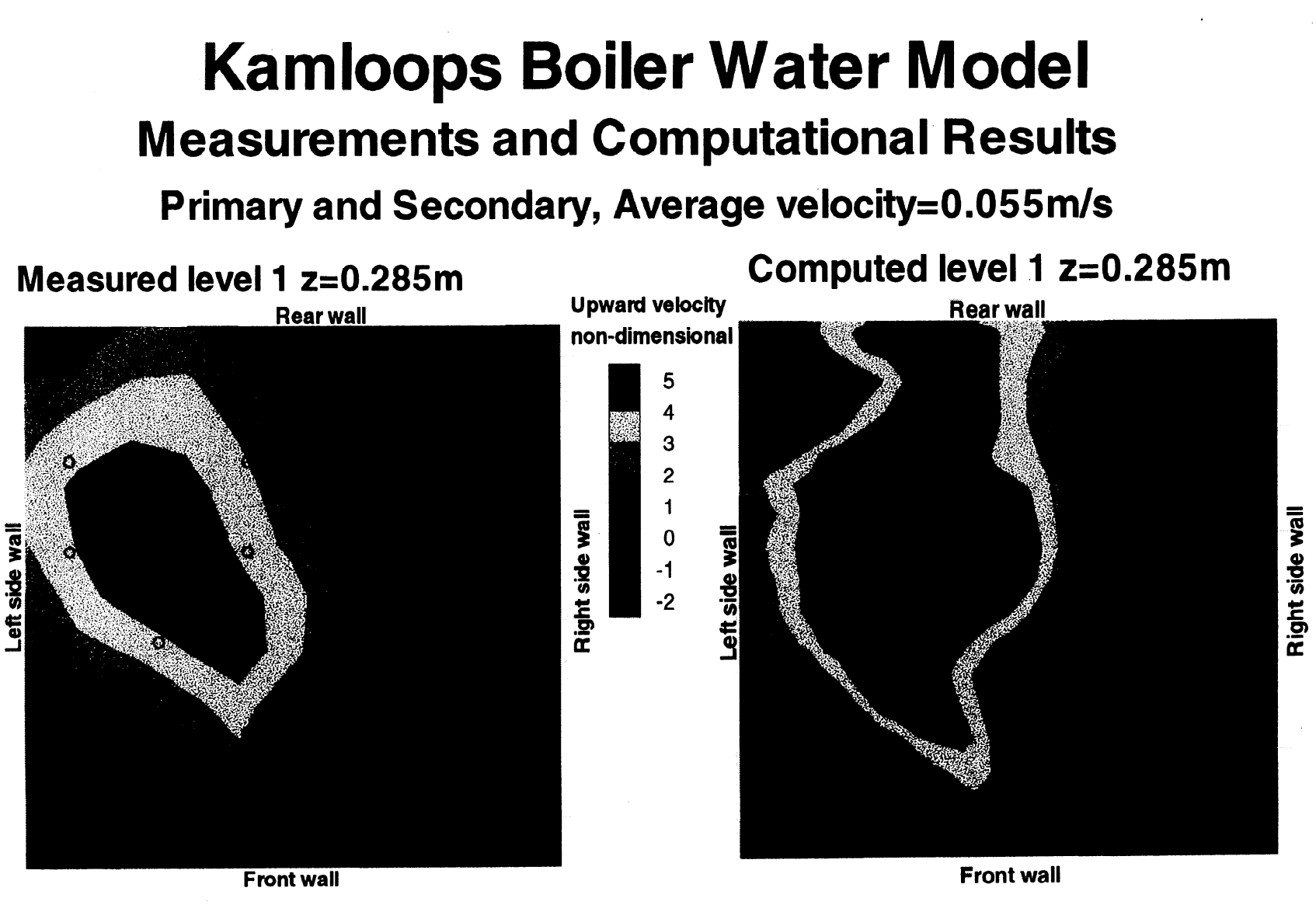

Figure 37. Measured and Computed Vertical Velocity Contours at Level 1.

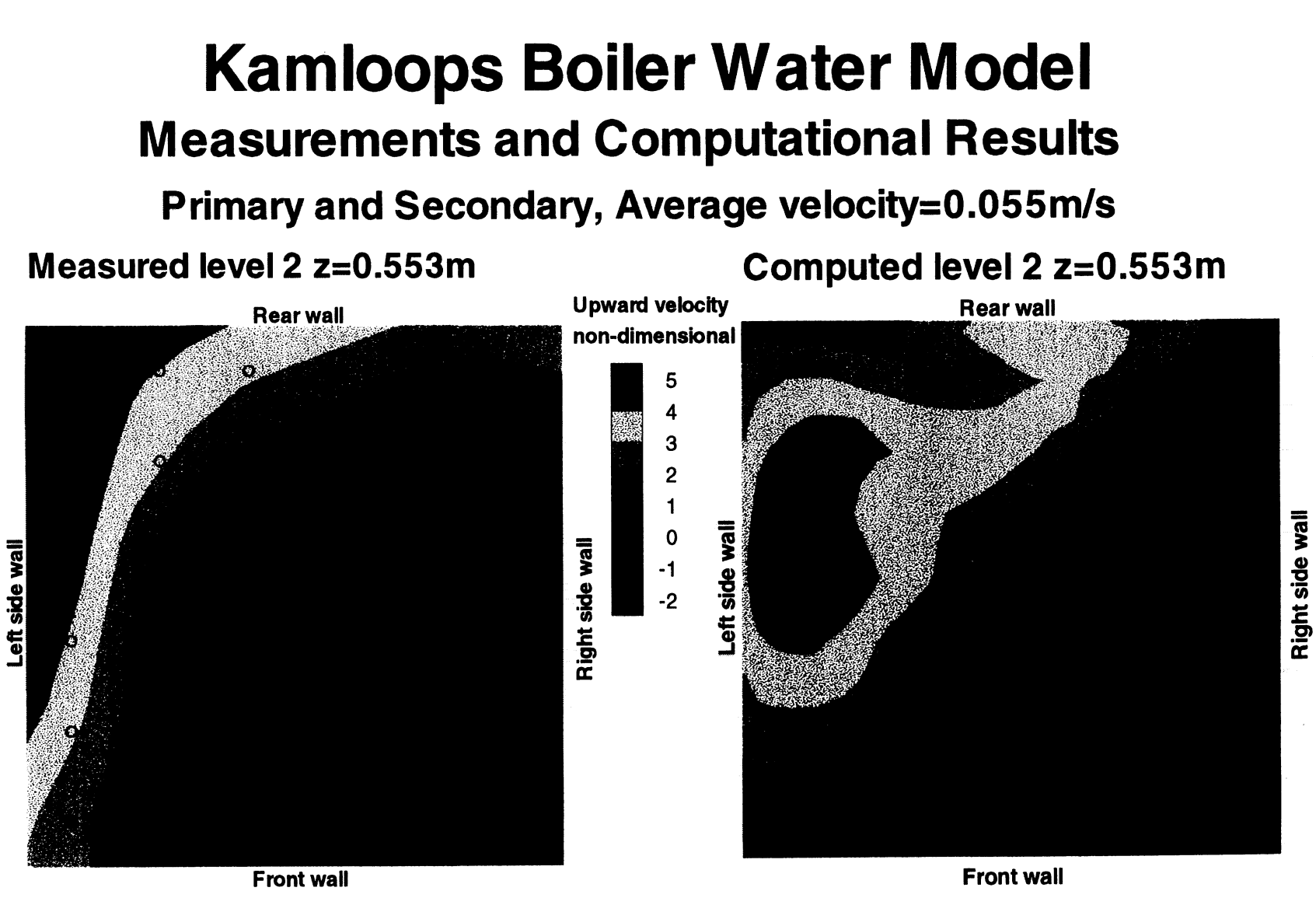

Figure 38. Measured and Computed Vertical Velocity Contours at Level 2.

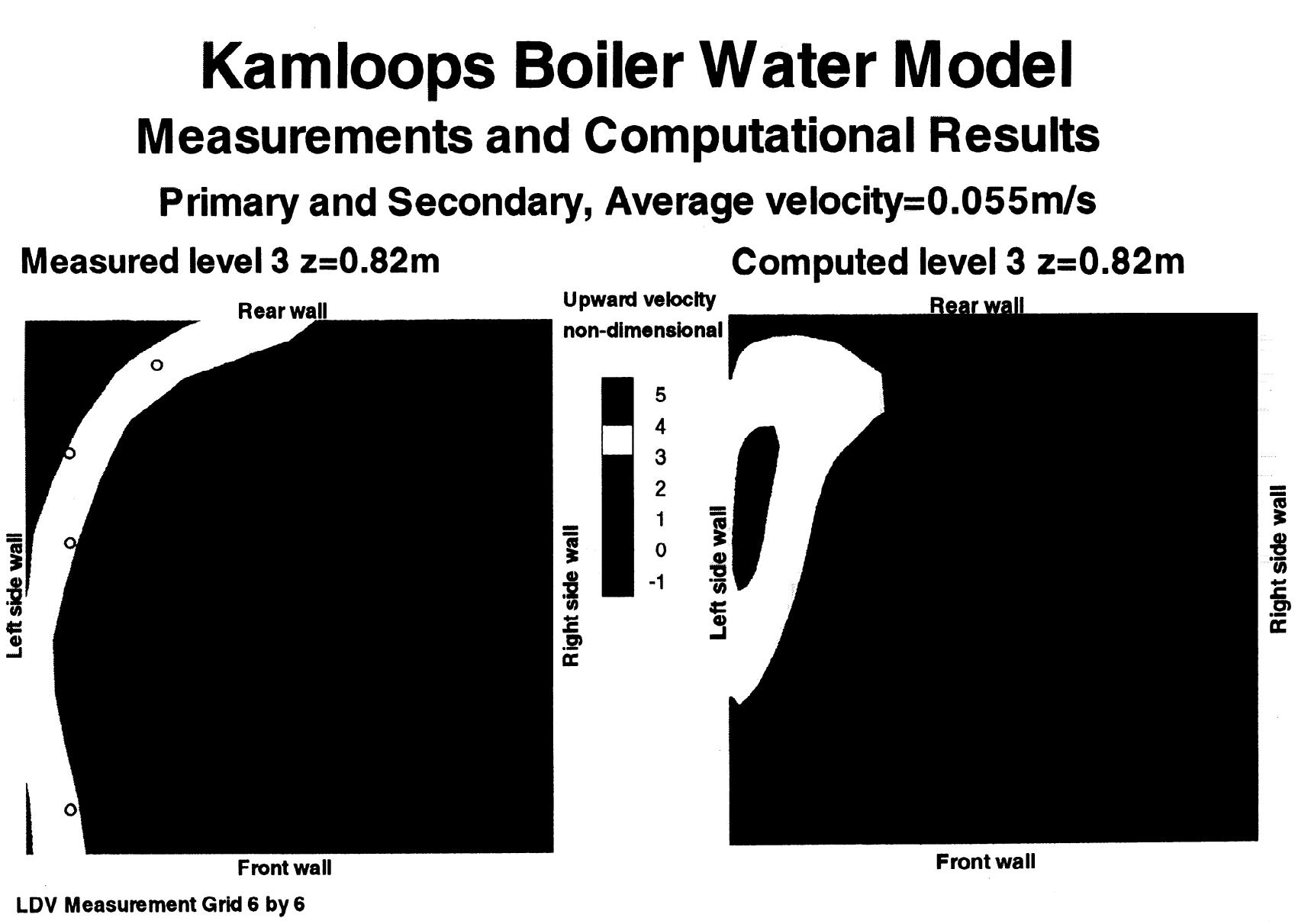

Figure 39. Measured and Computed Vertical Velocity Contours at Level 3.

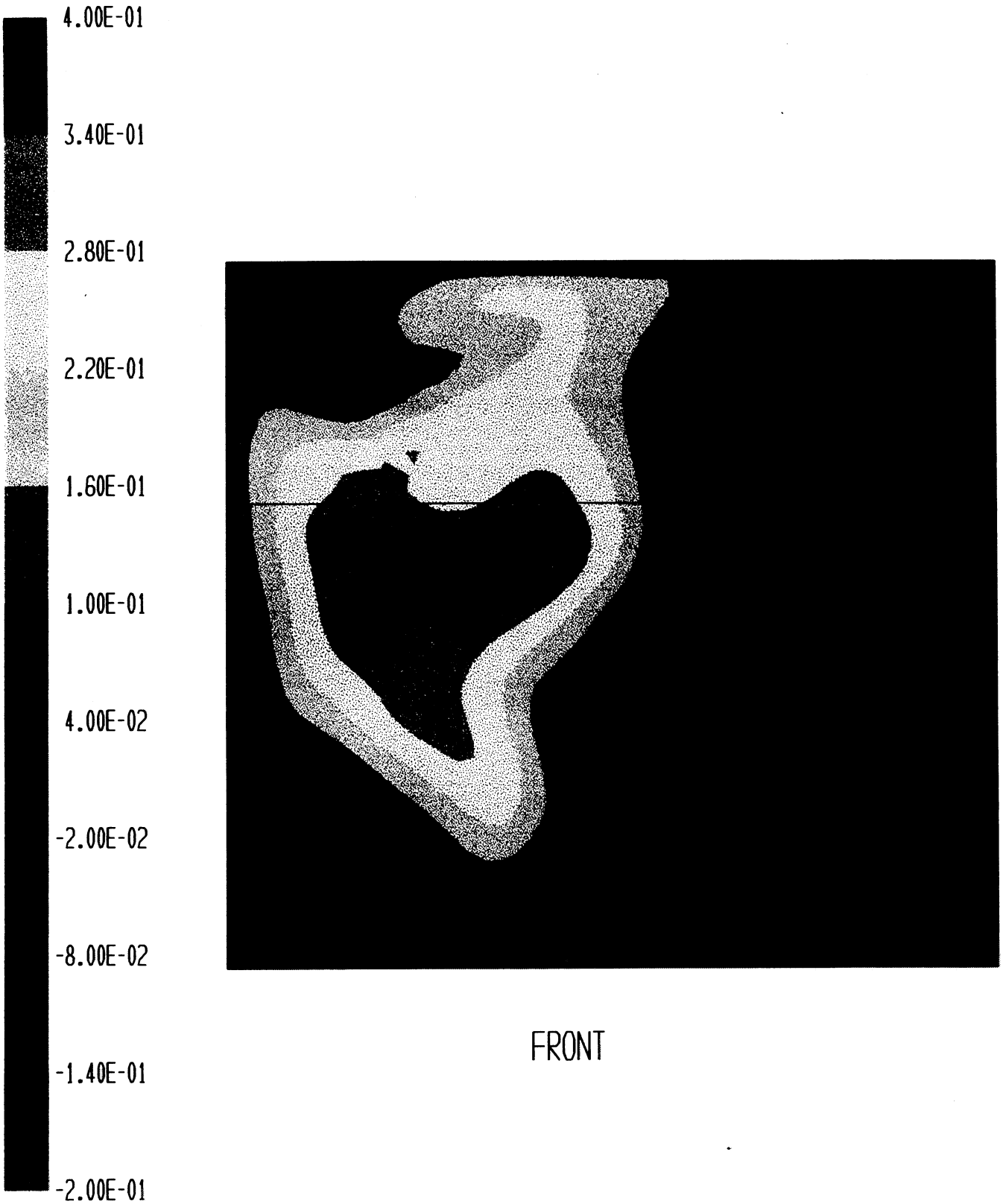

	Kamloops Recovery Boiler Water Model - KM2-2 w/ Sloped Floor	Sep 05 1997
	V-Velocity (Meters/Sec) LEVEL1 (J=30) 0.262M	Fluent 4.23
	Lmax = 4.000E-01 Lmin = -2.000E-01	Fluent Inc.

Figure 40. Fluent Model Computed Vertical Velocity Contours at Level 1.

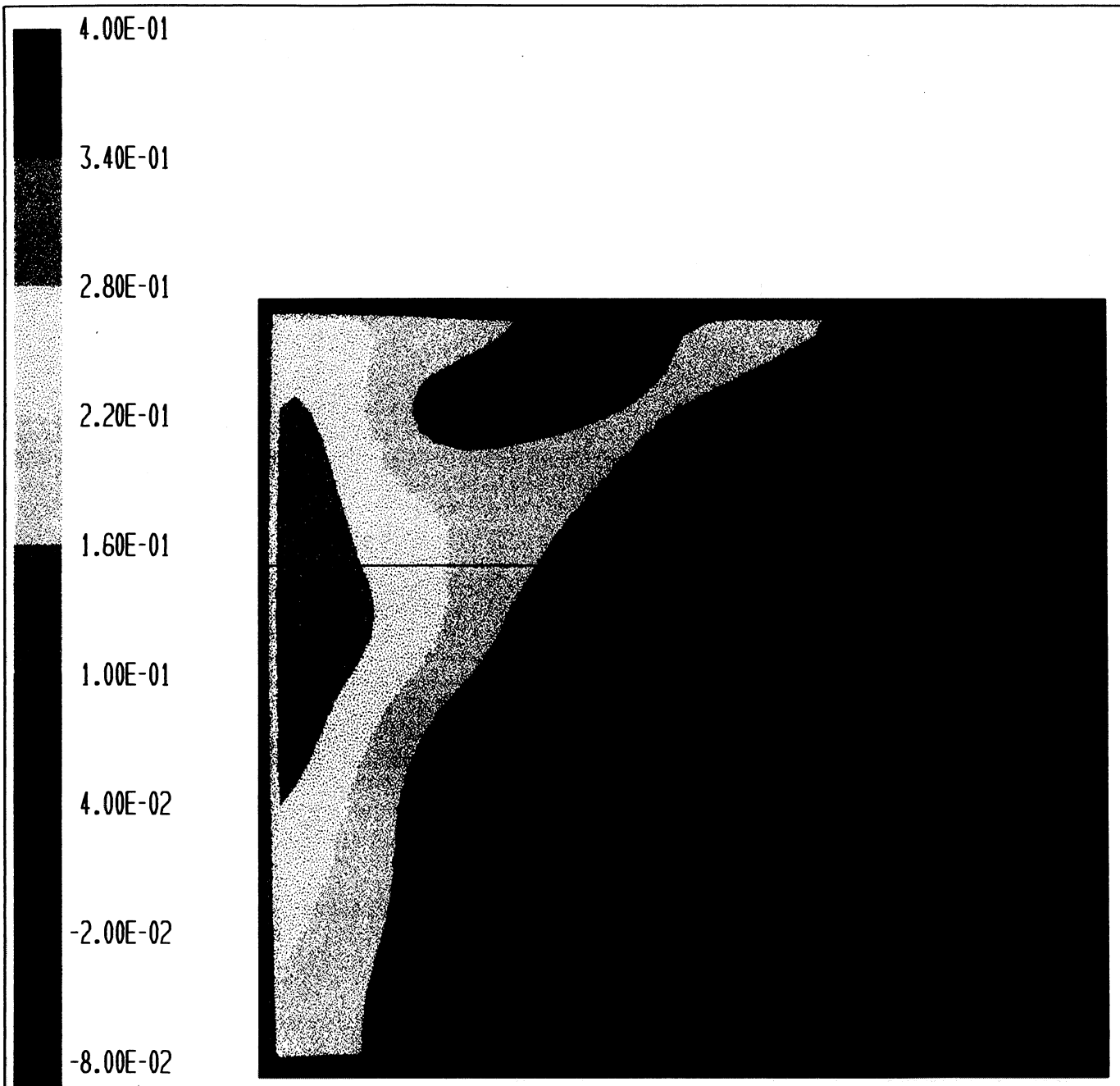

Kamloops Recovery Boiler Water Model - KM2-2 w/ Sloped Floor | Sep 05 1997
V-Velocity (Meters/Sec) LEVEL2 (J=35) 0.563M | Fluent 4.23
Lmax = 4.000E-01 Lmin = -2.000E-01 | Fluent Inc.

Figure 41. Fluent Model Computed Vertical Velocity Contours at Level 2.

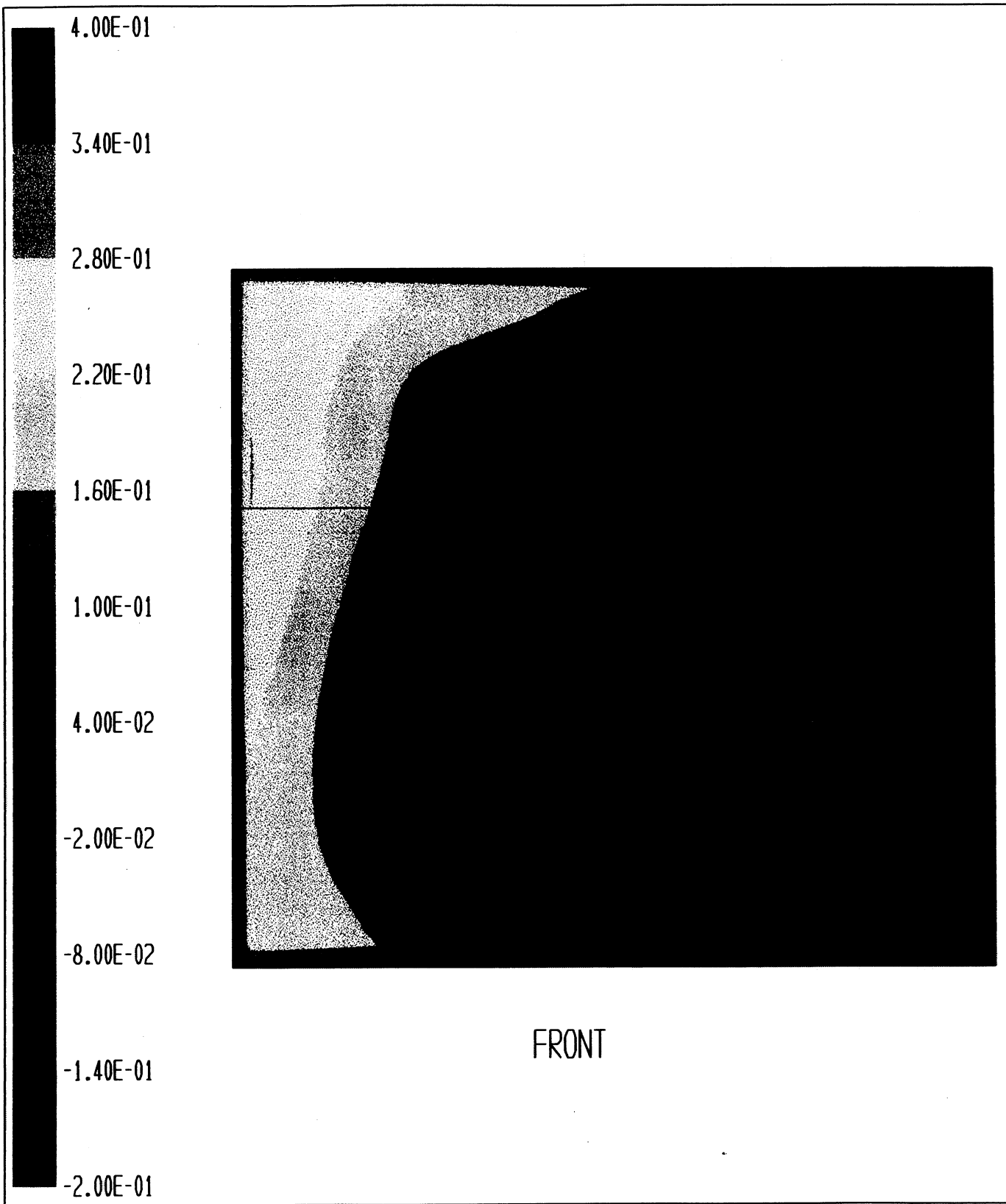

	Kamloops Recovery Boiler Water Model - KM2-2 w/ Sloped Floor	Sep 05 1997
	V-Velocity (Meters/Sec) LEVEL3 (J=38) 0.816M	Fluent 4.23
	Lmax = 4.000E-01 Lmin = -2.000E-01	Fluent Inc.

Figure 42 Fluent Model Computed Vertical Velocity Contours at Level 3.